Bone morphogenetic protein 2 induces pulmonary angiogenesis via Wnt–β-catenin and Wnt–RhoA–Rac1 pathways

Vinicio A. de Jesus Perez,[1] Tero-Pekka Alastalo,[3] Jenny C. Wu,[1] Jeffrey D. Axelrod,[2] John P. Cooke,[1] Manuel Amieva,[3] and Marlene Rabinovitch[3]

[1]Department of Medicine, [2]Department of Pathology, and [3]Department of Pediatrics, Stanford University, Stanford, CA 94305

Mutations in bone morphogenetic protein (BMP) receptor II (BMPRII) are associated with pulmonary artery endothelial cell (PAEC) apoptosis and the loss of small vessels seen in idiopathic pulmonary arterial hypertension. Given the low penetrance of BMPRII mutations, abnormalities in other converging signaling pathways may be necessary for disease development. We hypothesized that BMPRII supports normal PAEC function by recruiting Wingless (Wnt) signaling pathways to promote proliferation, survival, and motility. In this study, we report that BMP-2, via BMPRII-mediated inhibition of GSK3-β, induces β-catenin (β-C) accumulation and transcriptional activity necessary for PAEC survival and proliferation. At the same time, BMP-2 mediates phosphorylated Smad1 (pSmad1) or, with loss of BMPRII, pSmad3-dependent recruitment of Disheveled (Dvl) to promote RhoA–Rac1 signaling necessary for motility. Finally, using an angiogenesis assay in severe combined immunodeficient mice, we demonstrate that both β-C– and Dvl-mediated RhoA–Rac1 activation are necessary for vascular growth in vivo. These findings suggest that the recruitment of both canonical and noncanonical Wnt pathways is required in BMP-2–mediated angiogenesis.

Introduction

Bone morphogenetic proteins (BMPs) are members of the TGF-β superfamily of proteins that coordinate cell proliferation, differentiation, and survival in embryogenesis and adult tissue homeostasis (Attisano and Wrana, 2002). BMP-2, -4, and -7 exert their biological effects by interacting with serine/threonine kinase receptors BMP receptor IA (BMPRIA; ALK3) or BMPRIB (ALK6) and their coreceptor, BMPRII. Downstream signaling events include the phosphorylation of Smad1/5/8, interaction with comediator Smad4, nuclear translocation, and gene transcription. Although many of the biological effects of the BMPs have been related to the Smad-dependent pathways, Smad-independent MAPK pathways (JNK, p38, and extracellular receptor-dependent kinase 1/2 [ERK1/2]) also play an active role in BMP signaling (Massague, 2003).

Given the range of biological functions controlled by BMP signaling, much effort has been directed at understanding how dysfunction in this pathway contributes to the development of disease. Idiopathic pulmonary arterial hypertension (PAH [IPAH]) is a disease linked to aberrant BMPRII function. Different heterozygous loss of function mutations in BMPRII are observed in 25% of sporadic and 70% of familial cases of IPAH in which the penetrance is only 20% (Deng et al., 2000; Thomson et al., 2000; Machado et al., 2001). However, reduced BMPRII expression is observed in patients with IPAH without a BMPRII mutation and with the more common acquired forms of PAH, e.g., related to a congenital heart defect (Roberts et al., 2004).

IPAH is a rare condition (one to two newly diagnosed cases per million people per year) with a predilection for young

Correspondence to Marlene Rabinovitch: marlener@stanford.edu

Abbreviations used in this paper: ActR, activin receptor; β-C, β-catenin; BMP, bone morphogenetic protein; BMPR, BMP receptor; Dvl, Disheveled; EC, endothelial cell; ERK, extracellular receptor-dependent kinase; hPAEC, human PAEC; IPAH, idiopathic PAH; LEF, lymphoid enhancer binding factor; LIMK, LIM domain kinase; NLK, NEMO-like kinase; PAEC, pulmonary artery EC; PAH, pulmonary arterial hypertension; pERK, phosphorylated ERK; pSmad, phosphorylated Smad; SCID, severe combined immunodeficient; SMC, smooth muscle cell; TCF, T cell–specific transcription factor; Wnt, Wingless; WT, wild type.

The Rockefeller University Press $30.00
J. Cell Biol. Vol. 184 No. 1 83–99
www.jcb.org/cgi/doi/10.1083/jcb.200806049

women (female/male ratio of 2.3:1) and a median age at diagnosis of 36.4 yr (Rich et al., 1987). In the absence of treatment, IPAH patients have a mean survival of 2.8 yr (Massague, 2003; Humbert et al., 2004a). Both IPAH and the more common acquired forms of PAH are characterized by a progressive increase in pulmonary vascular resistance, attributed to the loss of small peripheral pulmonary arteries resulting from apoptosis of endothelial cells (ECs; Teichert-Kuliszewska et al., 2006) and occlusion of larger proximal pulmonary arteries resulting from the proliferation of smooth muscle cells (SMCs) and deposition of the extracellular matrix. In the late stages of the disease, in and around some of these occluded vessels, aberrant EC channels can be found reflecting the expansion of apoptosis-resistant EC populations (Tuder and Voelkel, 2002) that may arise from endogenous or circulating progenitor cells (Asosingh et al., 2008). Current therapies include oral and intravenous agents with vasodilatory properties that improve symptoms but do not reverse or consistently prevent the progression of the disease, leaving lung transplantation, with its inherent high mortality and morbidity, as the only choice for patients with the end-stage disease (Humbert et al., 2004b).

Work in transgenic animals has facilitated our understanding of the link between aberrant BMP signaling and pulmonary vascular pathology. Homozygous deletion of BMPRII (Beppu et al., 2000) and BMPRIA (Mishina et al., 1995) results in lethality during gastrulation, whereas mice heterozygous for BMPRII are relatively normal but can develop more severe pulmonary hypertension and vascular remodeling when exposed to high levels of serotonin (Long et al., 2006) or when injected with lipoxygenase (Song et al., 2005).

Experiments performed in human pulmonary artery ECs (PAECs [hPAECs]) show that the loss of BMPRII by RNAi impairs the ability of BMP-2 to enhance PAEC survival under proapoptotic conditions (Teichert-Kuliszewska et al., 2006). However, hPAECs cultured from patients with IPAH and documented BMPRII mutations exhibit enhanced proliferation compared with ECs from healthy donors (Masri et al., 2007), and this may account for the aberrant angiogenesis within the lumen and the adventitia of the vessels with plexogenic obstructive arteriopathy observed in advanced IPAH. However, cells from the IPAH patients are impaired in their ability to form tubelike structures in culture (Masri et al., 2007), and this may be responsible for their inability to reconstitute the lost distal pulmonary vascular bed. Thus, a comprehensive understanding of normal regulation of EC function by BMPRII signaling is a necessary first step in appreciating how abnormalities lead to disease.

An interaction between BMPs and members of the Wingless (Wnt) signaling pathway is implicated in embryonic lung development, as both BMP and Wnt signaling cascades coordinate stem cell fate determination and commitment to lung branching morphogenesis (Chen et al., 2005). In other organs, BMPs (Deckers et al., 2002; Langenfeld and Langenfeld, 2004; Chen et al., 2005; Raida et al., 2005) and Wnts (Ishikawa et al., 2001; Masckauchan et al., 2005) participate in angiogenesis associated with development and disease.

Wnts can signal through a canonical β-catenin (β-C)–dependent pathway via interaction with a receptor complex composed of a Frizzled protein and low density lipoprotein receptor–related protein family member (LRP5 or 6). The cytoplasmic protein Disheveled (Dvl) is recruited, facilitating inhibition of GSK3-β. This protects β-C from ubiquitination and allows it to accumulate in the cytoplasm and shuttle to the nucleus, where it interacts with other transcription factors and activates genes involved in cellular maintenance, proliferation, and survival such as c-myc, cyclin D1, VEGF, survivin, and axin2 (Bain et al., 2003; Rawadi et al., 2003; Logan and Nusse, 2004; Chen et al., 2005). Wnts can also activate noncanonical (i.e., non β-C dependent) signaling, the best studied of which is the Wnt–RhoA–Rac1 pathway involved in tissue polarity (Axelrod and McNeill, 2002) and in coordinated cell movement during embryological development (Habas et al., 2003).

In this study, we show that BMP-2 recruits canonical and noncanonical Wnt signaling pathways to promote PAEC proliferation, survival, and migration. Canonical β-C–mediated signals require BMP-2 activation of phosphorylated ERK (pERK) to mediate GSK3-β inactivation, whereas noncanonical signaling involves BMP-2 activation of phosphorylated Smad1 (pSmad1) to recruit Dvl and activate RhoA and Rac1. The canonical pathway depends on BMP-2–BMPRII interaction, whereas in the absence of BMPRII, BMP-2 can still promote motility by signaling through activin receptor IIa (ActRIIa) to mediate pSmad3 recruitment of Dvl to the RhoA–Rac1 pathway. Finally, we extend our observations to an in vivo model of angiogenesis and show, using a Matrigel plug assay in severe combined immunodeficient (SCID) mice (Skovseth et al., 2007), that BMP-2 stimulates angiogenesis in a β-C– and Dvl-dependent manner.

Results

BMP-2 and Wnt3a induce proliferation, migration, and survival of hPAECs

Based on a previous study (Langenfeld and Langenfeld, 2004), we chose to use BMP-2 as a ligand to investigate BMPRII signaling in hPAECs. Endogenous production of Wnt1, -2, -3a, -4, -9a, and -16 in PAECs was documented using a semiquantitative RT-PCR to screen for all 19 Wnt family members (Fig. S1, available at http://www.jcb.org/cgi/content/full/jcb.200806049/DC1). Our decision to use Wnt3a in our experiments was based on its ability to activate both canonical (Nusse and Varmus, 1992) and noncanonical (Endo et al., 2005) signaling pathways. We first starved hPAECs for 24 h in 0.1% serum, added 10 ng/ml BMP-2 or 100 ng/ml Wnt3a, and measured cell counts after 24 h. 50 ng/ml VEGF-treated cells and cells exposed to 0.1% serum were used as positive and negative controls, respectively. Both BMP-2 and Wnt3a significantly increased hPAEC cell counts (Fig. 1 A). To test the effect of the same ligands on hPAEC survival, cells were serum starved for 24 h and exposed for a further 24 h to serum-free conditions in the presence or absence of BMP-2 or Wnt3a. Caspase 3/7 assays indicate that both BMP-2 and Wnt3a reduce apoptosis when compared with vehicle-treated controls (Fig. 1 A). To investigate whether BMP-2 or Wnt3a also stimulates hPAEC migration, cells were seeded

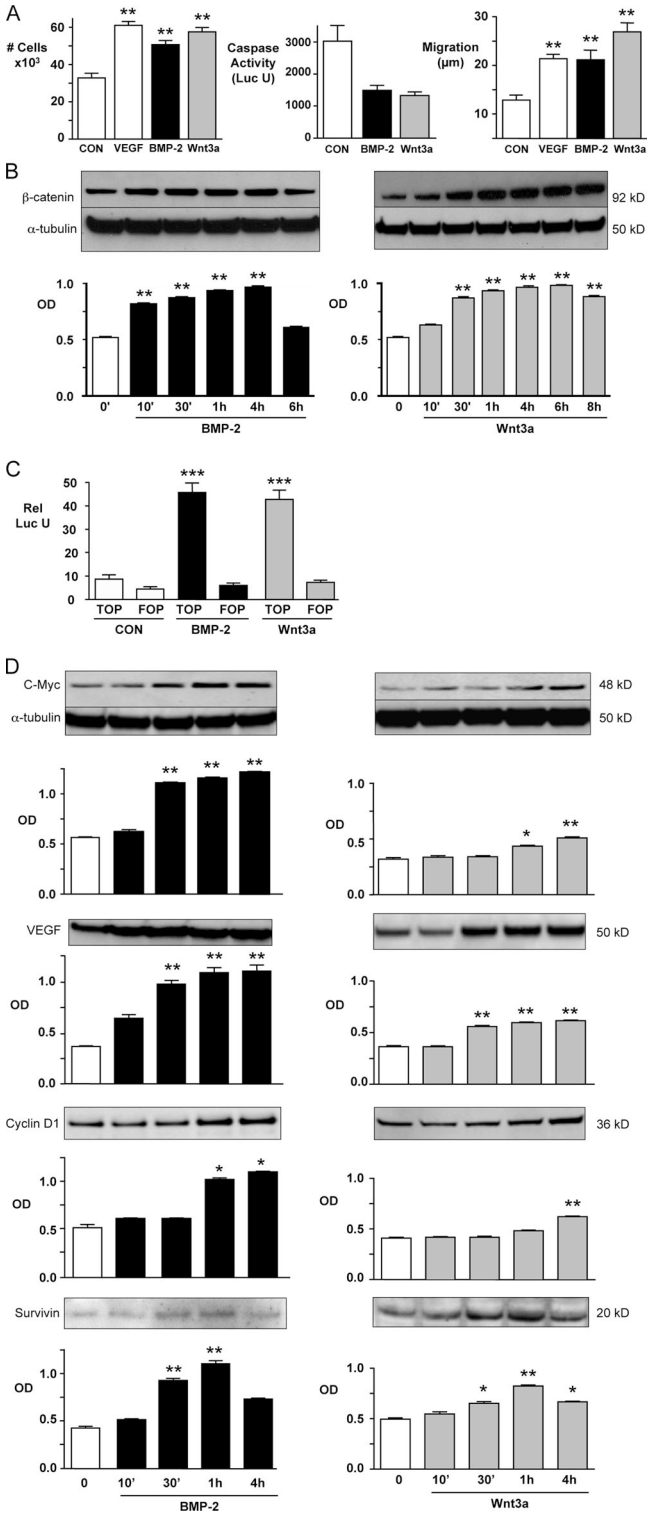

Figure 1. **BMP-2 and Wnt3a promote proliferation, migration, and survival of hPAECs while increasing β-C transcriptional activity and target genes.** (A) Cell count, caspase 3/7 apoptosis, and microcarrier bead migration assays of hPAECs in the presence or absence of 10 ng/ml BMP-2 or 100 ng/ml Wnt3a. Serum-free conditions were used to induce apoptosis, whereas 50 ng/ml of recombinant human VEGF was used as a positive control for proliferation and motility. (B) Representative Western immunoblots (top) and densitometry values (bottom) for β-C normalized to α-tubulin in response to BMP-2 and Wnt3a stimulation as in A. (C) TOPflash luciferase assays. hPAECs were transfected with TOPflash or FOPflash (negative control) luciferase reporter plasmids or Renilla (control for transfection efficiency). 6 h after stimulation with BMP-2 and Wnt3a, lysates were analyzed for luciferase activity relative to Renilla. CON, control. (D) Representative immunoblots for c-myc, VEGF, cyclin D1, and survivin in lysates of hPAEC stimulated with Wnt3a or BMP-2 as described in A. Values were normalized for α-tubulin. Error bars represent mean ± SEM from four different experiments performed in triplicate. *, $P < 0.01$; **, $P < 0.001$; ***, $P < 0.0001$ (vs. unstimulated control).

onto Cytodex 3 carrier beads and embedded in vitronectin gels in the presence of BMP-2 or Wnt3a for 48 h. Both BMP-2 and Wnt3a promoted hPAEC migration in a manner similar to that seen with VEGF, the positive control, judged by the distance migrated from the beads (Fig. 1 A).

BMP-2 and Wnt3a promote β-C–mediated transcriptional activity in hPAECs

Wnt3a is associated with canonical β-C signaling in a variety of cells, including ECs (Wright et al., 1999). Given the similarities in biological responses in hPAECs, we proposed that BMP-2, like Wnt3a, could activate β-C signaling to induce the expression of Wnt target genes. Immunoblots using an antibody that recognizes the active nonphosphorylated form of β-C were performed on lysates from hPAECs stimulated for 6 or 8 h with BMP-2 or Wnt3a. We observed that both agonists induce a significant increase in the level of active β-C within 10–30 min of stimulation (Fig. 1 B). Using confocal microscopy, increased levels of nuclear β-C were demonstrated in BMP-2–stimulated hPAECs within 1 h (Fig. S2, available at http://www.jcb.org/cgi/content/full/jcb.200806049/DC1). To relate the observed increase in active β-C to changes in target gene transcription, we nucleofected cells with the lymphoid enhancer binding factor (LEF)/T cell–specific transcription factor (TCF) promoter-reporter construct (TOPflash) or with the negative control plasmid (FOPflash) followed by measurement of luciferase. After 6 h of stimulation, luciferase was significantly elevated in TOPflash-transfected hPAECs stimulated with either BMP-2 or Wnt3a when compared with unstimulated or FOPflash-transfected cells (Fig. 1 C).

Next, we related the Wnt3a- and BMP-2–induced increase in β-C transcriptional activity to downstream gene targets that could be implicated in the functional changes observed. Immunoblots were performed using antibodies for VEGF 121, c-myc, cyclin D1, and survivin, given their established role in EC proliferation, survival, and migration (He et al., 1998; Tetsu and McCormick, 1999; Zhang et al., 2001a,b). Lysates obtained up to 4 h after stimulation with either agonist showed an increase in the levels of these proteins (Fig. 1 D).

Reduction of β-C decreases BMP-2– and Wnt3a-induced hPAEC proliferation and survival but enhances migration

Because BMP-2 and Wnt3a increase β-C transcriptional activity and target proteins potentially involved in hPAEC proliferation, survival, and migration, we next determined whether β-C was necessary for these functions. hPAECs were nucleofected with siRNA duplexes designed against β-C, which achieved an ~75% knockdown of total β-C protein 24 h after

transfection (Fig. 2 A). Cell counts (Fig. 2 B) show that β-C siRNA–treated hPAECs failed to exhibit the increased proliferative response to BMP-2 and Wnt3a compared with hPAECs transfected with nontargeting siRNA. Our survival experiments showed that the loss of β-C reversed the survival advantage induced by BMP-2 and Wnt3a in response to serum deprivation (Fig. 2 C). However, the loss of β-C enhanced BMP-2– and Wnt3a-mediated motility (Fig. 2 D). These findings raised the possibility that both Wnt3a and BMP-2 could be simultaneously activating a β-C–independent pathway necessary for cell motility.

BMPRII knockdown reduces proliferation and survival but promotes migration

Mutations in BMPRII in IPAH result in loss of expression and function (Humbert et al., 2004a). To study the biological impact of BMPRII deficiency on hPAEC proliferation, migration, and survival, we performed knockdown experiments using a pool of siRNA designed against the BMPRII sequence and achieved an ∼75% reduction in protein levels at 24 h (Fig. 3 A). This was also associated with a reduction in TOPflash activity under baseline conditions and in response to BMP-2 (Fig. 3 B).

In the setting of BMPRII knockdown, hPAECs failed to proliferate in response to BMP-2 when compared with controls. However, when hPAECs were stimulated with Wnt3a or VEGF, BMPRII knockdown had no significant effect on proliferation (Fig. 3 C). Similarly, the protection against apoptosis conferred by BMP-2 was lost with the knockdown of BMPRII, but this did not affect the response to Wnt3a (Fig. 3 D). However, the loss of BMPRII, similar to the loss of β-C, resulted in an increase in BMP-2– but not Wnt3a-mediated hPAEC motility (Fig. 3 E).

Therefore, we performed experiments to (a) address how BMP-2 via BMPRII might be stimulating β-C gene regulation to influence proliferation and survival and (b) establish how BMP-2 can regulate cell motility by using a β-C–independent pathway.

BMP-2 increases β-C via BMPRII-dependent pERK1/2 inhibition of GSK3-β

The regulation of β-C levels in mammalian cells is largely dependent on targeted phosphorylation by GSK3-β followed by ubiquination and proteasomal degradation (Logan and Nusse, 2004). GSK3-β can be inactivated by targeted phosphorylation of serine 9 or 21, allowing the accumulation of β-C (Cohen and Frame, 2001). Several kinase pathways are known to inhibit GSK3-β, among which IP3/Akt, p38, and ERK1/2 are the best studied (Cohen and Frame, 2001; Ding et al., 2005; Thornton et al., 2008). Given that BMPs are known to activate these same pathways through Smad-independent mechanisms (Sugimori et al., 2005; Jin et al., 2006), we investigated whether BMP-2–mediated activation of Akt, ERK1/2, and p38 occurred in hPAECs concomitant with GSK3-β inactivation. We observed no change in the BMP-2–mediated phosphorylation of Akt and p38 (unpublished data) in contrast to a rapid induction of ERK1/2 phosphorylation. To determine whether BMP-2 via BMPRII mediates pERK1/2 and whether pERK1/2 is necessary for β-C accumulation and transcriptional activity, we

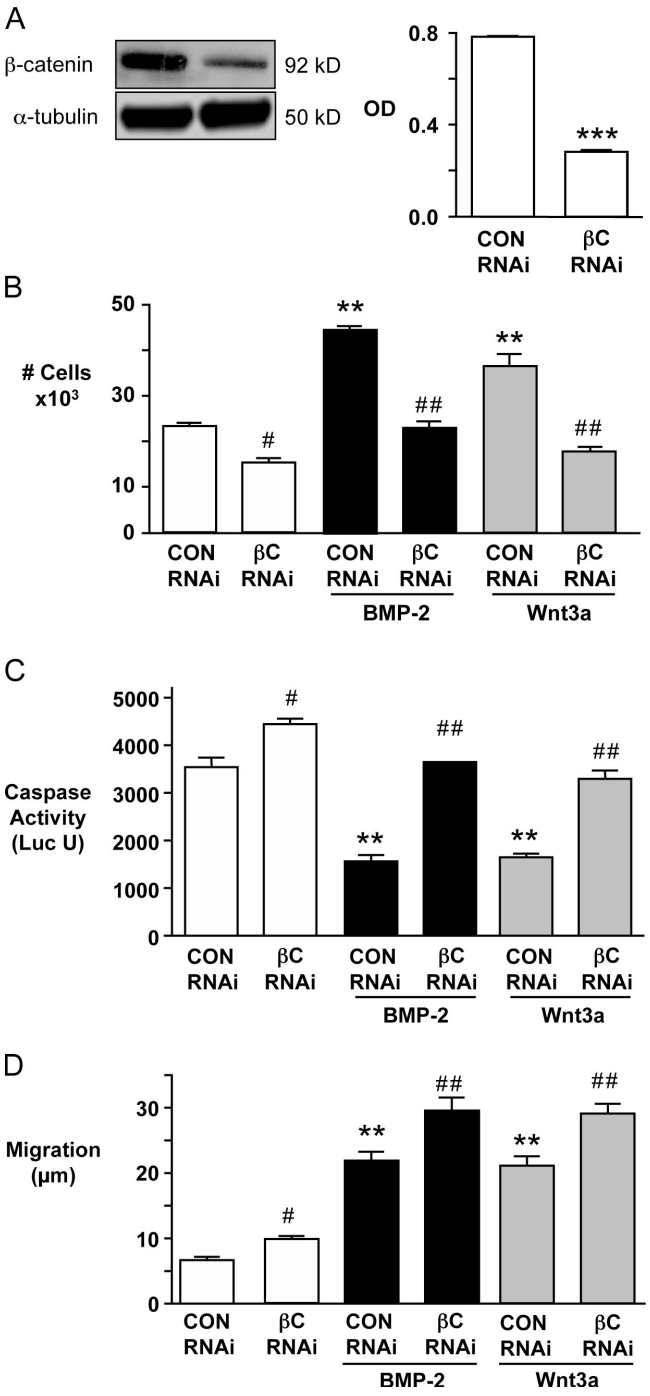

Figure 2. **Knockdown of β-C reduces the proliferation and survival response of hPAECs to BMP-2 and Wnt3a but enhances their migratory response.** (A) Western immunoblots for β-C and α-tubulin of hPAECs nucleofected with nontargeting control (CON RNAi) and β-C–specific siRNA (βC RNAi). ***, $P < 0.0001$ (compared with nontargeting control). (B–D) Cell proliferation (B), caspase 3/7 activity (C), and cell migration (D) assays using cells nucleofected with nontargeting or β-C–specific siRNA were performed as in Fig. 1. Error bars represent mean ± SEM from three different experiments performed in triplicate. **, $P < 0.001$ (BMP-2 or Wnt3a vs. unstimulated nontargeting control); #, $P < 0.01$ and ##, $P < 0.001$ (β-C–specific siRNA vs. corresponding nontargeting control).

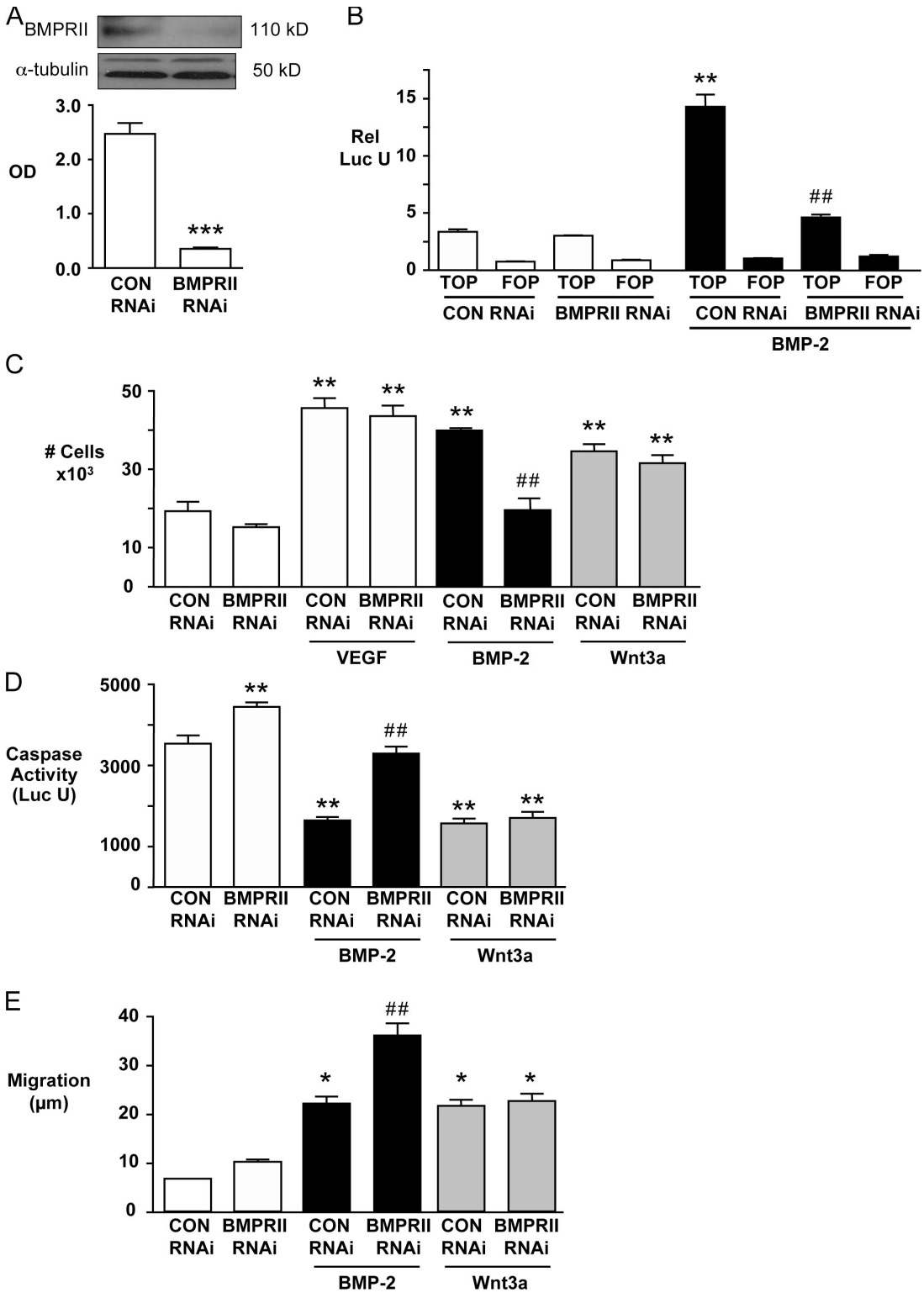

Figure 3. **Knockdown of BMPRII reduces BMP-2–mediated proliferation and survival of hPAECs but enhances their migratory response.** (A) Western immunoblots for BMPRII and α-tubulin in hPAECs nucleofected with nontargeting control (CON RNAi) and BMPRII siRNA (BMPRII RNAi). Error bars denote mean ± SEM for three different assessments. ***, $P < 0.0001$ (vs. nontargeting control). (B) TOPflash activity assay. **, $P < 0.001$ (vs. nontargeting control); ##, $P < 0.001$ (vs. BMP-2–stimulated nontargeting control). (C–E) Cell proliferation (C), caspase 3/7 activity (D), and cell migration (E) assays using cells nucleofected with nontargeting or BMPRII-specific siRNA as in Fig. 1. (B–E) Error bars represent mean ± SEM from three different experiments performed in triplicate. *, $P < 0.01$ and **, $P < 0.001$ (vs. unstimulated nontargeting control); ##, $P < 0.001$ (vs. BMP-2– or Wnt3a–stimulated nontargeting control).

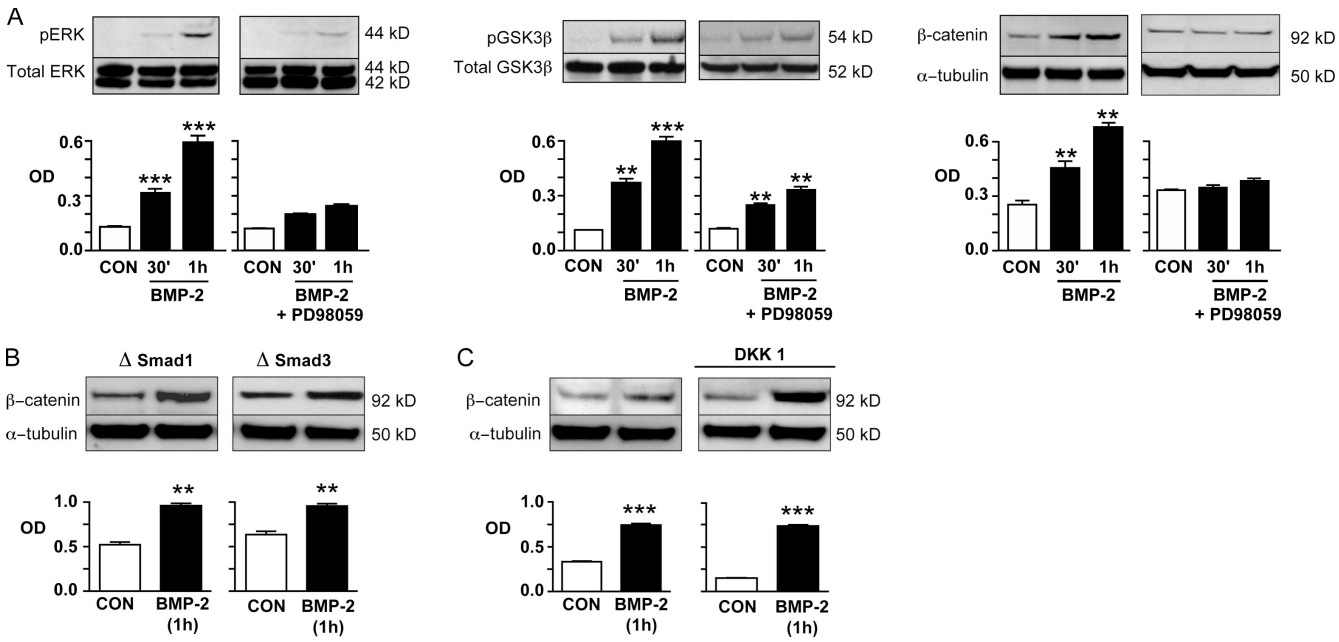

Figure 4. **BMP-2 activation of β-C transcriptional activity in hPAECs is dependent on ERK.** (A) Western immunoblots of hPAECs stimulated with BMP-2 in the presence or absence of 10 μM PD98059. Blots were probed for pERK, total ERK, GSK3-β, and β-C. (B) Western immunoblots of hPAECs transfected with dominant-negative (Δ) Smad1 or -3 constructs and stimulated with 10 ng/ml BMP-2 for 1 h. Blots were probed for active β-C and α-tubulin as a loading control (CON). (C) Western immunoblots of hPAECs incubated with 10 ng/ml BMP-2 in the presence or absence of 500 ng/ml DKK 1 for 1 h. Blots were probed for active β-C and α-tubulin as a loading control. Error bars denote mean ± SEM for three different experiments performed in triplicate. **, $P < 0.001$ and ***, $P < 0.0001$ (vs. control).

stimulated control and BMPRII siRNA–treated hPAECs with BMP-2 for 1 h. The coincidental increase in pERK1/2 with phosphorylation (i.e., inactivation) of GSK3-β and subsequent accumulation of β-C was abrogated in cells treated with BMPRII siRNA (Fig. S3, available at http://www.jcb.org/cgi/content/full/jcb.200806049/DC1). As a control, we showed that hPAECs treated with BMPRII siRNA responded to Wnt3a stimulation by an increase in both β-C and TOPflash transcriptional activity (unpublished data).

To determine a requirement for pERK1/2 in the regulation of GSK3-β activity, we incubated hPAECs with BMP-2 in the presence of PD98059, a known inhibitor of the ERK1/2 pathway. We show that BMP-2 fails to activate ERK1/2 when PD98059 is present and that this is associated with both a lack of GSK3-β phosphorylation and accumulation of β-C (Fig. 4 A). Similar results were obtained using a dominant-negative (Δ) ERK construct (adenoviral vector containing a FLAG-tagged ERK2-AEF construct with mutated phosphorylation sites; Fig. S4 A, available at http://www.jcb.org/cgi/content/full/jcb.200806049/DC1). The lack of β-C accumulation with BMP-2 stimulation also correlated with suppressed β-C transcriptional activity, as indicated by reduced TOPflash reporter activity in the presence of PD98059 (Fig. S4 B).

Although BMP-2–mediated β-C activation appears to be dependent on ERK1/2 activation, we also investigated the potential contribution of pSmads (Labbe et al., 2000) and/or autocrine Wnt signaling (Fischer et al., 2002) in this process. We found that BMP-2–mediated β-C accumulation in hPAECs transfected with either a dominant-negative (Δ) Smad1 or Smad3 construct in a manner similar to that of vector-only transfected hPAECs (Fig. 4 B). To address whether BMP-2 might be mediating β-C accumulation through the production and extracellular release of Wnts, we treated hPAECs with 500 ng/ml DKK 1. DKK 1 interacts with LRP 5/6 to interfere with receptor complex formation and Wnt-induced signal transduction (Glinka et al., 1998). There was no reduction in the BMP-2–induced accumulation of β-C in either carrier or DKK 1–treated hPAECs (Fig. 4 C).

BMP-2 and Wnt3a activate GTPases RhoA and Rac1

Although our aforementioned findings indicate that BMP-2 via BMPRII can recruit β-C to regulate proliferation and survival of hPAECs, they do not explain the BMPRII- and β-C–independent mechanism involved in BMP-2–mediated hPAEC motility. As shown in one study, Wnt3a can signal via the β-C–independent RhoA–Rac1 pathway to coordinate embryological events such as gastrulation (Habas et al., 2003). In CHO and neuronal cells, this pathway promotes cytoskeletal changes that facilitate cell migration through the formation of lamellipodia and filopodia (Boutros et al., 1998; Habas et al., 2003; Kishida et al., 2004; Endo et al., 2005). Activation of the Wnt–RhoA–Rac1 pathway leads to targeted induction of downstream proteins like LIM domain kinase (LIMK) and ROCK I/II, which are involved in stabilization of the actin cytoskeleton and actin–myosin contraction, respectively (Yang et al., 1998; van Nieuw Amerongen and van Hinsbergh, 2001; Sandquist et al., 2006).

Using pull-down assays to precipitate the active forms of RhoA and Rac1, we showed a significant increase in active RhoA and Rac1 over a 4-h period in hPAECs stimulated with both

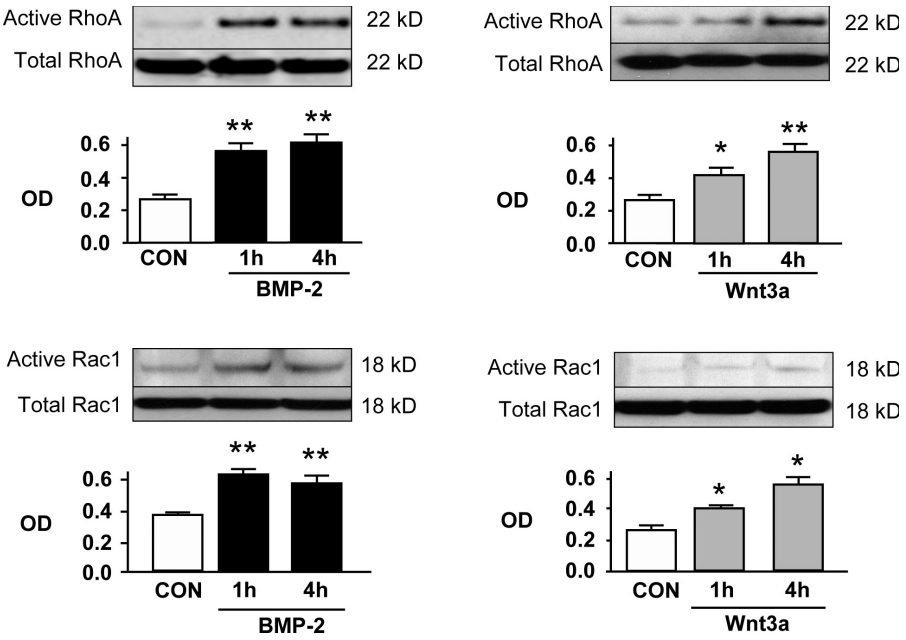

Figure 5. **BMP-2 and Wnt3a increase levels of active RhoA and Rac1 in hPAECs.** Active RhoA and Rac1 pull-down experiments were performed on hPAECs starved for 24 h followed by incubation with 10 ng/ml BMP-2 or 100 ng/ml Wnt3a for 1 and 4 h. Representative immunoblots for RhoA and Rac1 are shown along with densitometry. Levels of active RhoA and Rac1 were measured against total RhoA and Rac1 in cell lysates. Error bars denote mean ± SEM for three different experiments with triplicate assessments. *, $P < 0.01$ and **, $P < 0.001$ (vs. control [CON]).

BMP-2 and Wnt3a (Fig. 5). The activation of RhoA and Rac1 temporally coincided with the increase in β-C activity, supporting the concomitant use of both canonical and noncanonical signaling by BMP-2 and Wnt3a.

BMP-2 and Wnt3a activation of RhoA and Rac1 requires Dvl

Dvl is a necessary intermediate in the signaling of both canonical and noncanonical Wnt pathways (Boutros et al., 1998; Logan and Nusse, 2004). It appears that the selection of either signaling pathway is dependent on the availability of the specific Dvl domains DIX, PDZ, and DEP (Axelrod et al., 1998; Boutros et al., 1998; Li et al., 1999; Wang et al., 2006). Although DIX and PDZ are mainly involved in canonical signaling, DEP appears to be required in noncanonical functions (Axelrod et al., 1998; Boutros et al., 1998; Moriguchi et al., 1999; Wang et al., 2006). To show that RhoA and Rac1 activation in hPAEC is linked to BMP-2 via Dvl, we transfected GFP-tagged Dvl constructs containing various truncated versions of the protein (Fig. 6 A) and assessed their impact on RhoA–Rac1 activation. As shown in Fig. 6 (B and C), cells transfected with wild-type (WT) Dvl-GFP or ΔDIX Dvl-GFP show increased RhoA and Rac1 activity when stimulated with BMP-2. However, in ΔDEP Dvl-GFP–transfected cells, there is evidence of blunted RhoA activation and failure to activate Rac1. In DEP+ Dvl-GFP there is also no significant increase in RhoA with BMP-2 stimulation; although basal levels of active Rac1 are elevated, there is no further increase with BMP-2. This indicates that in addition to the DEP domain, the PDZ domain is necessary to activate normal RhoA–Rac1 activity in response to BMP-2.

We assessed cell motility in hPAEC transfected with the Dvl-GFP constructs seeded onto microcarrier beads and exposed to BMP-2 for 48 h. Cells carrying either the WT Dvl-GFP or ΔDIX Dvl-GFP construct exhibited a significant migratory response to BMP-2 compared with nonstimulated cells (Fig. 6 D). As predicted by our previous experiments, this did not occur in cells transfected with either DEP+ or ΔDEP Dvl-GFP. To show that the effects of the Dvl constructs were independent of β-C signaling, we probed the lysates of BMP-2–stimulated hPAECs transfected with each of the Dvl constructs for changes in β-C accumulation. We found no impairment in the β-C response under any experimental condition, providing further evidence that canonical signaling is not required for the modulation of hPAEC motility (Fig. S5 A, available at http://www.jcb.org/cgi/content/full/jcb.200806049/DC1).

BMP-2 mediates relocation of Dvl from the perinuclear region to the cell membrane

Several lines of evidence suggest that participation in RhoA–Rac1 signaling requires relocation of Dvl to the cell membrane to engage in signaling complexes (Yu et al., 2007). To provide evidence to support this feature in hPAECs, we used immunofluorescence and confocal microscopy to identify changes in Dvl after BMP-2 and Wnt3a stimulation and found that the distribution of Dvl changes to enter filopodia and lamellipodia after BMP-2 and Wnt3a stimulation (Fig. S5 B).

Confocal images of cells transfected with WT and mutant GFP-labeled constructs were used to examine the peripheral versus central localization of Dvl in response to BMP-2 stimulation and were quantified as described in Materials and methods (Fig. 6 E). After stimulation with BMP-2, both WT Dvl-GFP and ΔDIX Dvl-GFP (Fig. 6 E, green) extend into lamellipodia and filopodia and co-distribute with actin on the cell membrane (Fig. 6 E, yellow); i.e., a significant increase in peripheral to central distribution of Dvl is apparent. BMP-2–stimulated and nonstimulated hPAECs transfected with ΔDEP Dvl-GFP show discrete fluorescent granules in a perinuclear distribution with limited formation of lamellipodia (Fig. 6 E) and no peripheral redistribution. Cells transfected with the DEP+ Dvl-GFP construct show intense peripheral redistribution of Dvl on the cell

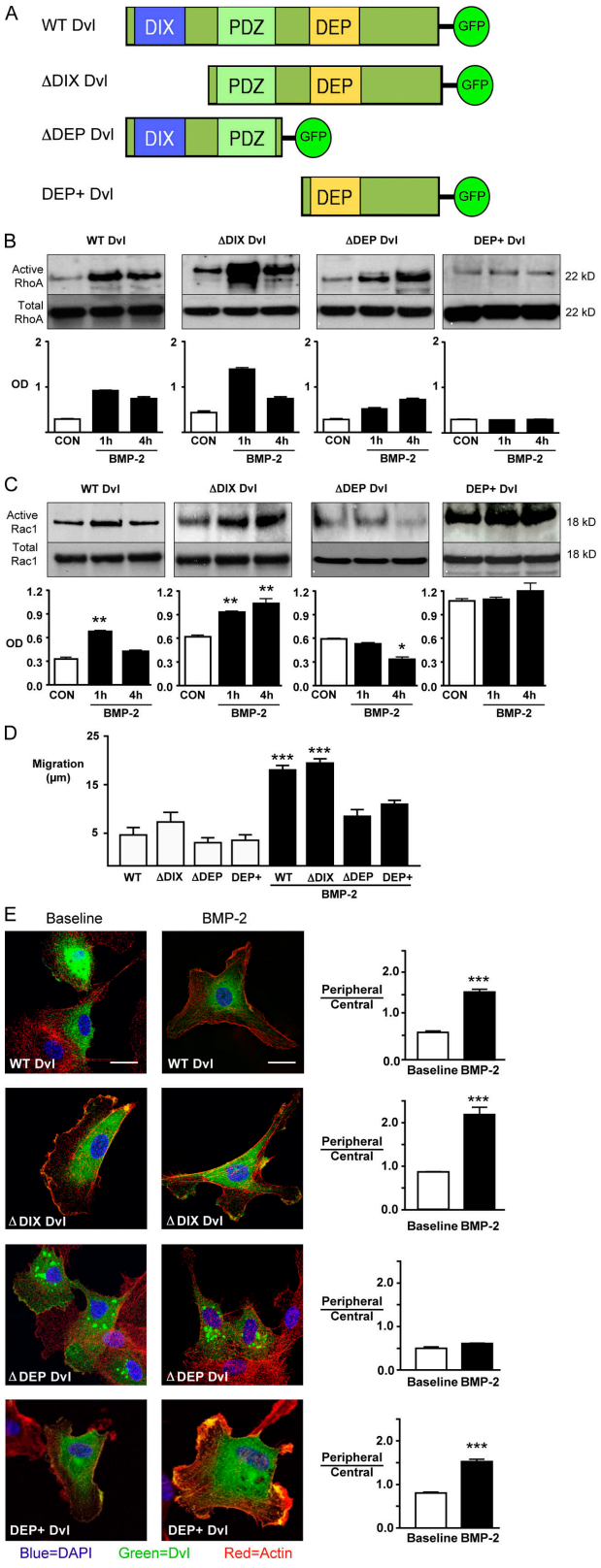

Figure 6. **BMP-2 recruits the PDZ and DEP domains of Dvl to activate RhoA and Rac1 and induce hPAEC motility.** (A) Diagram illustrating the structure of the four Dvl-GFP constructs used in the experiments described in this study. (B and C) Dvl constructs illustrated in A were individually nucleofected in hPAECs to assess impact on RhoA (B) and Rac1 (C) activation in the presence of 10 ng/ml BMP-2. Pull-down experiments were performed and analyzed as in Fig. 5. Error bars denote mean ± SEM for three different experiments with triplicate assessments. *, $P < 0.01$ and **, $P < 0.001$ (vs. control [CON]). (D) Microcarrier bead migration assay of hPAECs nucleofected with Dvl constructs and exposed to BMP-2 as in A. ***, $P < 0.0001$ (vs. WT and ΔDIX unstimulated). (E) Representative confocal images of hPAECs nucleofected with GFP-tagged Dvl constructs. Cells were starved for 24 h and incubated with BMP-2 as in B. Actin was labeled with Alexa Fluor 555–phalloidin (red), and nuclei were stained with DAPI (blue). Quantification of Dvl distribution in the cytoplasm and the periphery was performed as described in Materials and methods. ***, $P < 0.0001$ (vs. baseline). (D and E) Error bars denote mean ± SEM for three different experiments with quadruplicate assessments. Bars, 10 μm.

membranes, but the formation of lamellipodia is blunted, and filopodia are not observed.

Dvl relocation to lamellipodia and filopodia related to BMP-2–induced hPAEC motility

To show that Dvl relocation is required for BMP-2–induced hPAEC motility, hPAECs transfected with Dvl-GFP constructs were seeded in borosilicate sterile dual-chamber slides at a density of 15,000 cells per well. Using time-lapse video microscopy, we followed the movement of cells transfected with Dvl-GFP for >10 h. BMP-2–stimulated hPAECs moved faster and covered a larger distance compared with the unstimulated controls (Fig. 7, A and C). The captured images also show that in the presence of BMP-2, Dvl-GFP shifts to the migrating front end of the cells and concentrates at locations rich in filopodia and lamellipodia (Fig. 7 A and Videos 1 and 2, available at http://www.jcb.org/cgi/content/full/jcb.200806049/DC1). This feature is lost in the BMP-2–stimulated mutant ΔDEP Dvl-GFP–transfected cells (Fig. 7 B and Videos 3 and 4). These cells also fail to increase distance traveled and speed despite stimulation with BMP-2 (Fig. 7 C).

BMP-2 regulation of Dvl-induced RhoA and Rac1 motility is Smad1 dependent

It remained to be determined how BMP-2 can regulate Dvl-mediated activation of RhoA and Rac1. A recent study in bone marrow stromal cells has shown that Smad1, one of the three Smads associated with the BMP signaling, can interact with Dvl and suppress Wnt canonical activity by preferentially shuttling Dvl away from the proteins that promote the phosphorylation of β-C (Liu et al., 2006). Because BMP-2 mediates Smad1 activation in human aortic and umbilical venous ECs (Langenfeld and Langenfeld, 2004), we reasoned that in hPAECs, BMP-2 regulates Dvl activity via Smad1. Therefore, we transfected hPAECs with a construct encoding a dominant-negative Smad1 (ΔSmad1) and investigated whether this would interfere with BMP-2–mediated RhoA–Rac1 activation and motility. This Smad1 mutant contains a replacement of four amino acids, SSVS to AAVA, in exon 7 in the C terminus and thus cannot be phosphorylated; this same construct is also unable to bind to Dvl in immunoprecipitation assays (Liu et al., 2006). Pull-down assays show that in the setting of ΔSmad1, hPAECs stimulated by BMP-2 fail to activate RhoA or Rac1 (Fig. 8 A). Consistent with this observation, microcarrier bead assays show that hPAECs expressing ΔSmad1 also fail to

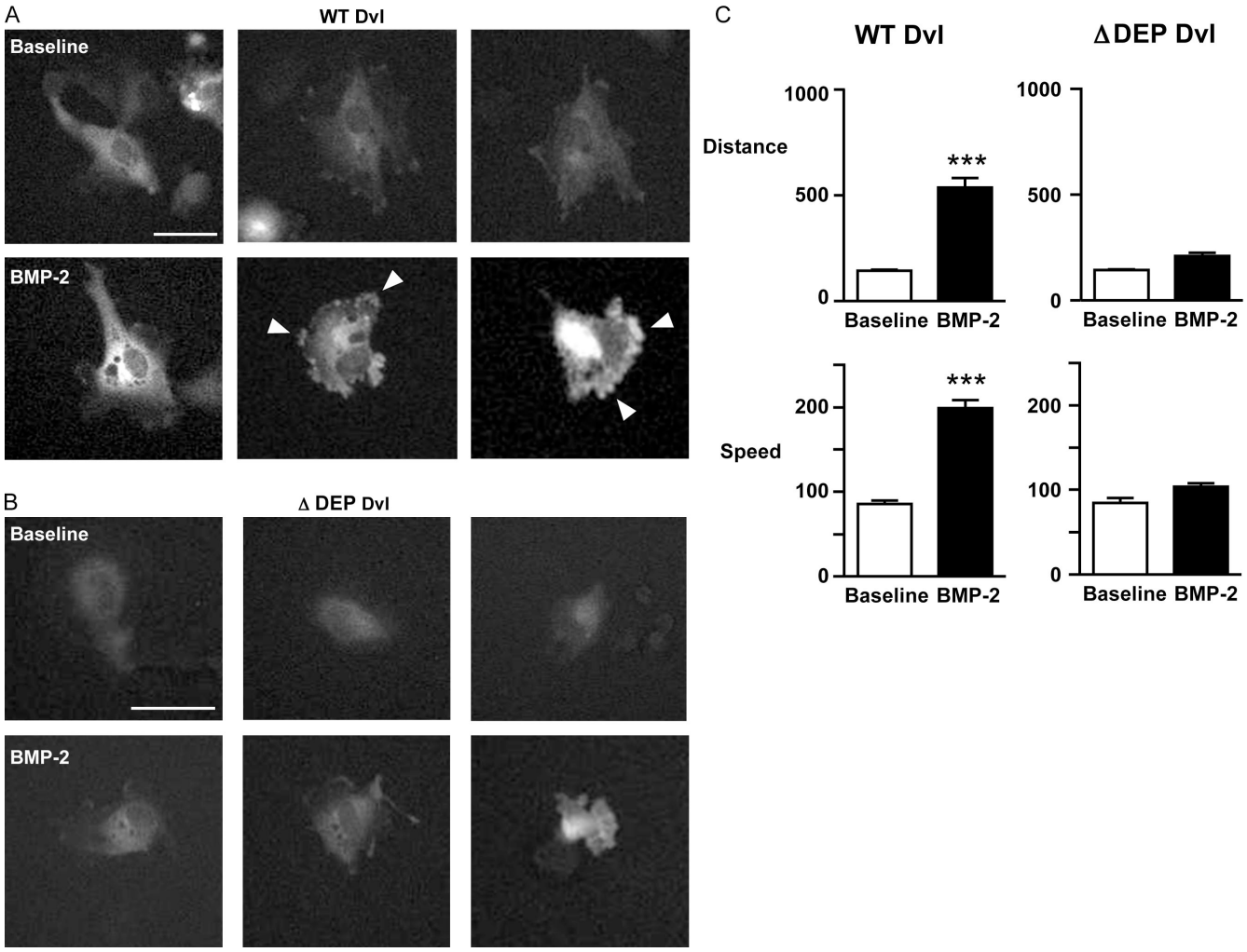

Figure 7. **BMP-2 facilitates redistribution of Dvl to filopodia and lamellipodia in hPAECs.** (A and B) Live images taken over a 10-h period of cells nucleofected with Dvl-GFP (A) or ΔDEP Dvl-GFP (B) and stimulated with either vehicle or 10 ng/ml BMP-2. Arrowheads indicate the marked presence of GFP signal in the migrating front end of Dvl-GFP–transfected cells incubated with BMP-2. See Videos 1–4 (available at http://www.jcb.org/cgi/content/full/jcb.200806049/DC1). (C) The distance and speed of control and BMP-2–stimulated cells transfected with Dvl-GFP and ΔDEP Dvl-GFP. Distance was measured by plotting the coordinates of the nuclei every 10 min for 10 h and adding the distance between the points. Speed was calculated by dividing the distance over time (10 h). Error bars denote mean ± SEM for three different experiments with triplicate assessments. ***, $P < 0.001$ (vs. baseline). Bars, 10 μm.

migrate in response to BMP-2 (Fig. 8 B), further supporting the need for functional Smad1.

BMP-2 promotes motility of BMPRII-deficient hPAECs by pSmad3 activation via ActRIIa, a member of the TGF-β receptor superfamily

In cells with reduced BMPRII, enhanced migration in response to BMP-2 suggested an alternate signaling pathway, resulting in increased noncanonical activity. Although Smad1/5/8 activation is markedly reduced in the setting of BMPRII mutations (Yang et al., 2005), BMPs can still signal in human pulmonary artery SMCs by recruiting BMPRIA and ActRIIa, another member of the TGF-β family of receptors (Yu et al., 2005). The ActRs are known to signal using Smad2 and -3. Moreover, Smad3 can interact with Dvl in mammalian cells (Warner et al., 2005). Therefore, we hypothesized that in the setting of reduced BMPRII availability, BMP-2 can still recruit Dvl by activating Smad3.

We show that in BMPRII-deficient cells, BMP-2 fails to activate pSmad1 but activates pSmad3 (Fig. 8 C). To link Smad3 activation with signaling through the alternate BMP-2 receptor ActRIIa, we cotransfected siRNA for BMPRII and ActRIIa (or a nontargeting control) into hPAECs and harvested cell lysates over 1 h. We achieved an 80% knockdown of ActRIIa, which is comparable with that for BMPRII (unpublished data). BMP-2–mediated activation of Smad3 is lost in cells deficient in both BMPRII and ActRIIa (Fig. 8 D).

To test the functional relevance of this alternate pathway in preserving BMP-2–mediated hPAEC migration, we transfected hPAECs with either a dominant-negative Smad3 (ΔSmad3) or an empty vector. This ΔSmad3 has been shown in one study to be unable to interact with Dvl or to be phosphorylated by TGF-β receptors (Warner et al., 2005). Microcarrier bead assays

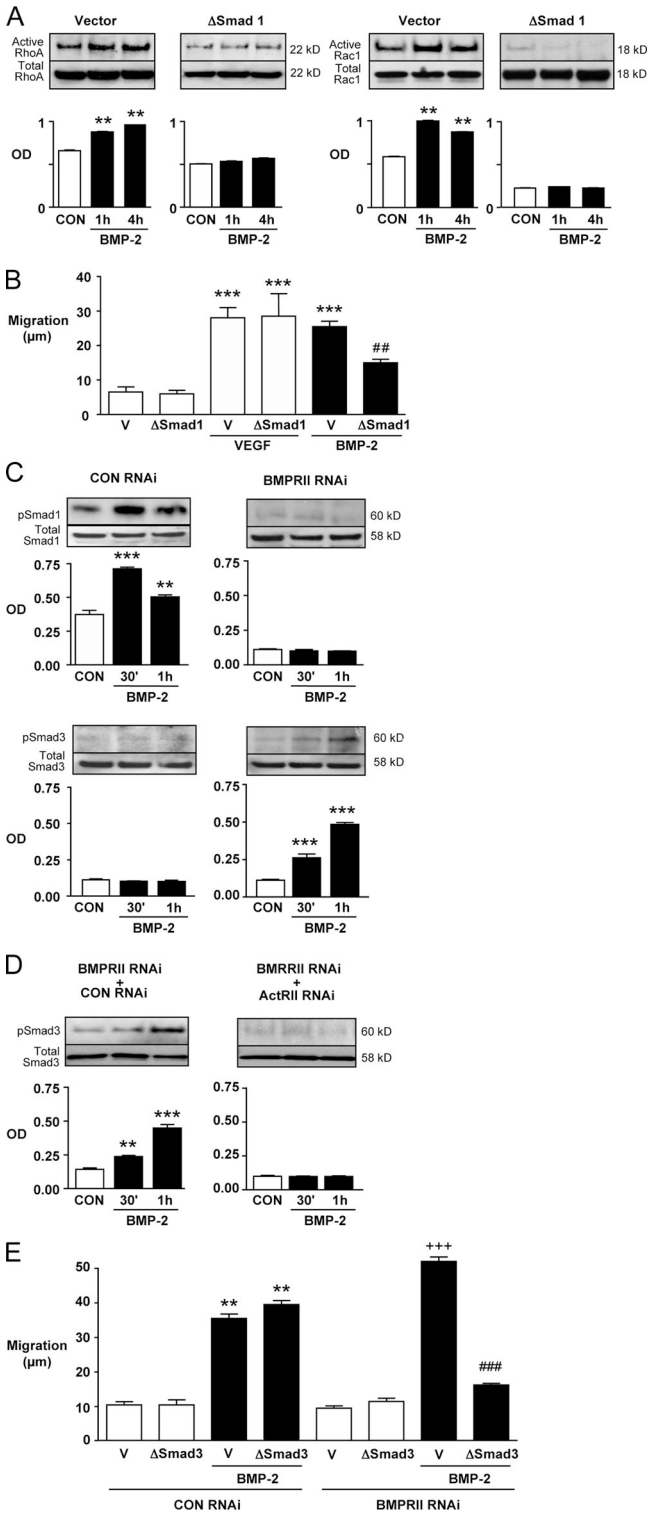

Figure 8. **Recruitment of Dvl by BMP-2 requires Smads and is independent of BMPRII functional status.** (A) Active RhoA and Rac1 pull-down experiments on hPAEC nucleofected with either vector or dominant-negative (Δ) Smad1 construct and incubated with 10 ng/ml BMP-2 were analyzed as described in Fig. 6. **, P < 0.001 (vs. control [CON]). (B) Microcarrier bead assay using hPAECs nucleofected with vector (V) or ΔSmad1 was performed as in Fig. 6 D. ***, P < 0.0001 (vs. control); ##, P < 0.001 (vs. vector only stimulated with BMP-2). (C) Western immunoblots of BMP-2–stimulated hPAECs transfected with BMPRII siRNA or nontargeting control siRNA. Blots were probed for phosphorylated and total Smad1 and -3. **, P < 0.001 and ***, P < 0.0001 (vs. control). (D) Western immunoblots of hPAECs transfected with siRNA for both BMPRII and ActRIIa followed by stimulation with 10 ng/ml BMP-2 for 1 h. Blots were probed for phosphorylated and total Smad1 and -3. **, P < 0.001 and ***, P < 0.0001 (vs. control). (E) Microcarrier bead assay using hPAECs nucleofected with BMPRII siRNA along with vector or dominant-negative Smad3 (ΔSmad3). **, P < 0.001 (BMP-2–stimulated vector or ΔSmad3 vs. respective unstimulated control RNAi); +++, P < 0.0001 (BMP-2–stimulated vs. unstimulated BMPRII RNAi vector or ΔSmad3); ###, P < 0.0001 (vector vs. ΔSmad3). Error bars denote mean ± SEM for three different experiments with triplicate assessments.

show that cells containing both BMPRII knockdown and ΔSmad3 failed to respond to BMP-2 stimulation, whereas those cells with BMPRII knockdown alone exhibited enhanced motility (Fig. 8 E). Thus, in the setting of reduced BMPRII, the activation of Smad3 by BMPRII-independent pathways compensates for reduced Smad1 signaling to preserve hPAEC motility.

BMP-2–mediated angiogenesis in SCID mice requires canonical and noncanonical Wnt pathways

Angiogenesis requires coordinated endothelial proliferation, migration, and alignment to form functional tubular structures (Adams and Alitalo, 2007). Current cell culture approaches cannot fully reproduce the complex biological environment where vessel growth occurs. For this reason, we applied a well-established angiogenesis assay to study the impact of BMP-2–mediated canonical and noncanonical signaling in the intact mouse (Skovseth et al., 2002, 2007). We implanted Matrigel plugs containing hPAECs transfected with either β-C siRNA or nontargeting siRNA into SCID mice and, 14 d later, assessed the formation of microvessels, the presence of murine–human hybrid endothelial tubes, and the number of murine and human ECs within the plugs (see Materials and methods). Compared with the baseline (Fig. 9, A and E), BMP-2–enriched Matrigel plugs (Fig. 9, B and F) containing hPAECs transfected with nontargeting siRNA exhibited greater numbers of both hPAECs and murine ECs (Fig. 9 I). In addition, vascular tubes comprised of both murine and human cells (mean of two tubes per 40× high power field) and microvessels containing red blood cells (mean of two to three microvessels per 40× high power field) were exclusively seen in this experimental group (Fig. 9, B and F). In contrast, BMP-2–enriched Matrigel plugs containing β-C–deficient cells (Fig. 9, C and G) showed neither hybrid microvessels nor an expansion of the hPAECs. Interestingly, in these plugs, the number of murine ECs increased in response to BMP-2 (Fig. 9 I).

To study the impact of dysfunctional noncanonical Wnt signaling on angiogenesis, we implanted Matrigel plugs containing hPAECs transfected with the dominant-negative Dvl construct ΔDEP into SCID mice. After 14 d, despite a significant murine and human EC growth response to BMP-2 compared with unstimulated controls, no evidence of microvessels or hybrid tube formation was found (Fig. 9, D, H, and J). Collectively, these experiments show that in vivo, BMP-2 stimulates an angiogenic response by recruiting canonical and noncanonical Wnt signaling pathways.

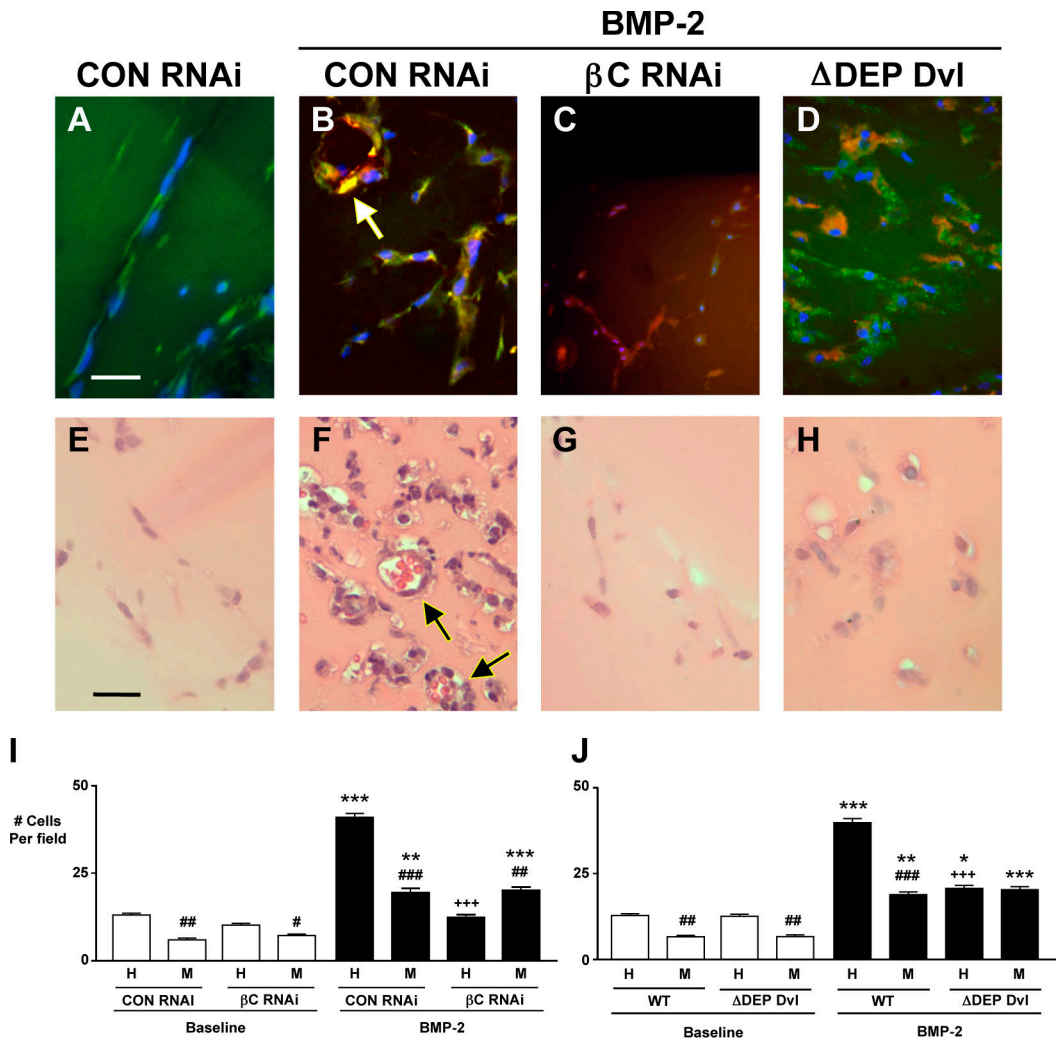

Figure 9. **Recruitment of both canonical and noncanonical signaling pathways is required for BMP-2–induced microvessel formation in SCID mice.** (A–H) Representative immunofluorescence (A–D) and H&E (E–H) images show the appearance of unstimulated (A and E) and BMP-2–stimulated (B and F) controls and β-C RNAi–treated (C and G) and ΔDEP Dvl–transfected (D and F) cells 14 d after implantation into SCID mice. Human and murine CD31 are labeled with green and red fluorescent antibodies, respectively, and nuclei are stained blue with DAPI. Hybrid vessels containing green and red ECs (B) in association with RBC-filled vessels (F) are seen under conditions of BMP-2 stimulation (arrows) but not when the hPAECs were transfected with β-C RNAi (C and G) or with ΔDEP (D and H). (I and J) Quantitative analysis of the mean number of human (H) and murine (M) cells found per 40× field. Comparisons are made between unstimulated control and β-C RNAi–treated (I) or ΔDEP-transfected (J) versus BMP-2–stimulated counterparts. Error bars denote mean ± SEM for four different experiments. *, $P < 0.01$; **, $P < 0.001$; ***, $P < 0.0001$ (vs. same lineage control [CON]; human or murine). ##, $P < 0.001$; ###, $P < 0.0001$ (human vs. murine). +++, $P < 0.0001$ (lineage-specific control vs. experimental [βC RNAi or ΔDEP]). Bars: (A–D) 10 µm; (E–H) 30 µm.

Discussion

The loss of small precapillary arteries is a feature of IPAH and secondary forms of PAH and is thought to result from injury and susceptibility of ECs to apoptosis. Previous studies have linked the loss of BMPRII to the development of IPAH and to the propensity of ECs to apoptose (Teichert-Kuliszewska et al., 2006; Masri et al., 2007). Our study looks into why that occurs and whether the same mechanisms might explain other features necessary for vascular regeneration, i.e., proliferation and migration. In this study, we report for the first time to our knowledge that a BMPRII ligand recruits a canonical Wnt signaling pathway to promote hPAEC survival and proliferation by activating ERK1/2 and stimulates a Dvl-mediated noncanonical RhoA–Rac1 pathway to induce migration by activating Smad1. Beyond uncovering mechanisms that relate to the loss of vessels in patients with IPAH, these findings may help better understand aberrant angiogenesis in disorders such as malignancy and may lead to new opportunities to stimulate the growth of new blood vessels in disease and in tissue regeneration.

The loss of ECs in larger arteries has been linked to the stimulation of SMC proliferation through the release of active TGF-β (Sakao et al., 2006). In addition, the emergence of apoptosis-resistant ECs that proliferate and migrate much more robustly than ECs of healthy donors (Masri et al., 2007) may account for the aberrant angiogenesis within the lumen and the adventitia of the vessels with plexogenic obstructive arteriopathy observed in advanced IPAH. However, cells from the IPAH patients are impaired in their ability to form tubelike structures in culture (Date et al., 2004; Masri et al., 2007), and this may account for their inability to reconstitute the lost distal pulmonary vascular bed. In unpublished data, we have evidence that

these apoptosis-resistant ECs may have constitutive signaling via β-C, as occurs with oncogenic β-C (Peifer, 1997).

Although our study shows that pERK1/2, and not pSmad1/5/8 or pSmad2/3, is necessary for β-C accumulation, it does not exclude the possibility that other signaling molecules activated or inhibited by BMPs might also play a role in mediating β-C accumulation. Besides pERK1/2 (Ding et al., 2005), BMPs can trigger Smad-independent signaling using kinase pathways such as JNK, which could also target GSK3-β for inhibition (Moule et al., 1997; Cohen and Frame, 2001; Ding et al., 2005). BMP signaling has also been shown to activate the MAPK TAK1 (Yamaguchi et al., 1995) that targets NEMO-like kinase (NLK), an endogenous inhibitor of canonical Wnt signaling that acts by interfering with DNA binding of the β-C–TCF transcriptional complex (Ishitani et al., 1999, 2003). Although our results support the ability of BMP-2 to enhance β-C activity in hPAECs, it may be possible that the BMP-TAK1-NLK axis may act to modulate transcriptional responses to prevent excessive gene expression and fine-tune biological effects. Further studies should be directed at investigating the extent to which kinases other than MAPK or regulation of the NLK-TAK1 axis can modulate the BMP-2–mediated activation of canonical Wnt signaling.

Previous work on BMP signaling has focused on the pSmad-dependent transcription of genes such as Indian hedgehog (Seki and Hata, 2004), Tlx2 (Tang et al., 1998), and inhibitor of differentiation (Miyazono and Miyazawa, 2002) that are involved in the regulation of cellular processes related to angiogenesis. The ability to activate β-C suggests that BMPs can induce a wider array of gene targets than previously considered. This is consistent with our finding that both BMP-2 and Wnt3a increase c-myc, VEGF, survivin, and cyclin D1, which are proteins that mediate hPAEC survival and proliferation. It is likely that the interaction between β-C and pSmad1/5/8 and perhaps other BMP-mediated transcription factors such as peroxisome proliferator–activated receptor γ (Hansmann et al., 2007) regulates the profile of expressed genes (Labbe et al., 2000; Hu and Rosenblum, 2005). It is also possible that there is a codependency between BMP and Wnt to limit the level of expression of gene targets when both agonists are present or to allow gene expression to persist despite loss of function mutations in BMPRII. Thus, haploinsufficiency of BMPRII may become more penetrant when there are concomitant alterations in Wnt signaling.

Directed migration is necessary for ECs to converge at sites where vessels need to be formed (Adams and Alitalo, 2007). Previous studies show that BMP-2 induces endothelial migration and vascular tube formation but without further investigation of the mechanisms involved (Deckers et al., 2002; Langenfeld and Langenfeld, 2004). Recent studies describing interactions between the cytoplasmic tail of BMPRII and proteins involved in the regulation of cytoskeletal dynamics such as LIMK (Foletta et al., 2003) and Tctex-1 (Machado et al., 2003) suggest a functional link between BMP signaling and cell motility. It would be of interest to investigate in future studies whether the interaction with the cytoskeleton and with LIMK is lost in BMPRII mutants, as no functional studies have yet linked this to changes in cell motility.

Our experiments showing heightened hPAEC migration in response to both BMP-2 and Wnt3a suggested that both ligands might be using a non–β-C–dependent Wnt signaling pathway. Wnt3a can recruit Dvl to activate RhoA and Rac1 (Kishida et al., 2004; Endo et al., 2005), which are small GTPases that coordinate features of cell motility (i.e., the cytoskeletal rearrangements that permit retraction of the base of the cell and extension of the leading front through the formation of lamellipodia and filopodia).

This study shows not only that Dvl is recruited by BMP-2 but that this process is pSmad dependent. The highly conserved PDZ and DEP domains in Dvl that were previously identified in *Drosophila melanogaster* as required for RhoA–Rac1 signaling and cell motility (Axelrod et al., 1998; Wang et al., 2006) are necessary for BMP-2 to induce hPAEC migration. Thus, a potential way in which pSmads could modulate the switch between canonical and noncanonical signaling would be through their ability to interact with the DIX domain of Dvl. This would limit the interaction of Dvl with protein partners necessary for β-C activation while exposing the PDZ and DEP domains to facilitate RhoA–Rac1 activation and cell motility.

How Dvl is partitioned between canonical and noncanonical signaling is not currently known, but it is possible that the interaction between Dvl and pSmads occurs in a different subcellular compartment segregating this pool of Dvl from that available for canonical activity. Consistent with this idea is the observation that Dvl accumulates either in vesicles (Capelluto et al., 2002) or associates with actin (Torres and Nelson, 2000).

An unexpected finding was that BMP-2 could control motility despite reduced BMPRII. We found that when BMPRII is lacking, BMP-2, using receptor complexes containing BMPRIA/B and the TGF-β superfamily receptor ActRIIa, signals via Smad2/3 to preserve motility in hPAECs. A similar interaction of BMPRIA with ActRIIa was observed with deletion of BMPRII in pulmonary arterial SMCs (Yu et al., 2005), but the functional consequences of the altered signaling were not investigated. Mutations in TGF-β receptors can also contribute to the development of PAH in patients with hemorrhagic hereditary telangiectasia (Cottin et al., 2007). However, whether mutations in other members of the TGF-β receptor superfamily compound the propensity to PAH when there is BMPRII loss of function is still unclear. In ECs isolated from plexogenic lesions, a reduction in TGF-β-RII was found, suggesting that abnormal signaling via this receptor may contribute to the development of vascular pathology (Yeager et al., 2001).

It would be of interest to further investigate the role of the planar cell polarity receptors in BMP-2– and Wnt3-mediated noncanonical Dvl–RhoA–Rac1 signaling to assess whether this pathway is important in establishing EC polarity and in recruiting pericytes and whether these particular features are BMPRII dependent. This pathway is critical in convergent extension; i.e., the medial convergence and intercalation of elongated mesenchymal cells along the anteroposterior axis that leads to elongation and narrowing of the body axis. Indeed, the orderly branching morphogenesis observed in normal angiogenesis in the lung and in other tissues strongly suggests that planar cell polarity signaling may be present (Lamalice et al., 2007).

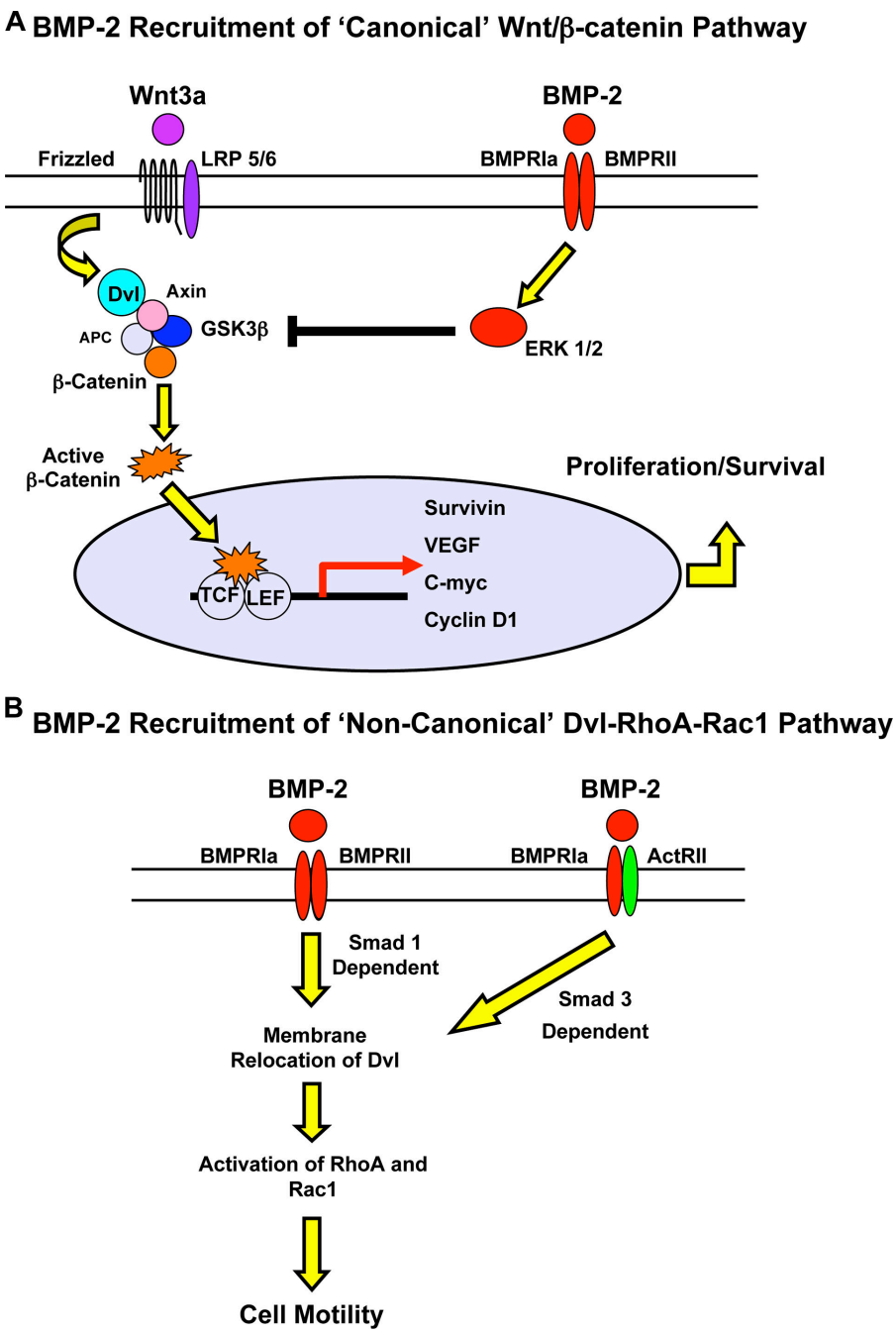

Figure 10. **Schema illustrating that regulation of proliferation, survival, and migration in hPAECs depends on cross talk between BMP and Wnt pathways.** (A) BMP-2 and Wnt3a promote an increase in β-C–mediated transcriptional activity and up-regulate gene targets involved in proliferation and survival. (B) However, migration is the result of a Smad1 or, with reduced BMPRII, a Smad3-dependent recruitment of Dvl, which allows selective activation of RhoA, Rac1, and downward targets involved with cytoskeletal reorganization and cell motility.

Fig. 10 illustrates our proposed models of how BMP-2 recruits canonical Wnt signaling to promote hPAEC growth and survival (Fig. 10 A) and noncanonical signaling to induce motility (Fig. 10 B). Our experiments are the first to show how BMPs regulate major EC functions required for normal angiogenesis by recruiting two Wnt signaling pathways. That BMP and Wnt signaling collaborate in angiogenesis is consistent with the observation that deletion of Frizzled 5 (Ishikawa et al., 2001) or targeted endothelial deletion of BMPRIA (unpublished data) result in early embryonic lethality associated with a profound defect in yolk sac vasculature. Although it is known that BMP can suppress Wnt5a (Suzuki et al., 2003), it now also should be considered that these ligands regulate common pathways fine-tuning gene expression and cellular function.

Materials and methods

Materials and reagents

Recombinant human BMP-2, α-tubulin antibody, protease inhibitor cocktail, and phosphatase inhibitor cocktail I and II were purchased from Sigma-Aldrich. PD98059 was obtained from EMD. Recombinant murine Wnt3a and human VEGF were bought from R&D Systems. FBS, PBS, MEM, optimized MEM, Medium 200, low serum growth supplement, gentamycin/amphotericin, polyvinylidene difluoride membranes, Lipofectamine 2000, Prolong Gold Antifade with DAPI, and Alexa Fluor 488– and 592–labeled antibodies were obtained from Invitrogen. Anti-VEGF and antisurvivin were obtained from Abcam. Anti-Dvl antibody was obtained from Santa Cruz Biotechnology, Inc. Anti–cyclin D1, Anti-pERK1/2 and –total ERK½, and GSK3-β were obtained from Cell Signaling Technology. Active β-C, Rac1, and RhoA antibodies, the TCF reporter assay system, and RhoA and Rac1 assay reagents were purchased from Millipore. Nucleofector II and reagents were purchased from Amaxa, Inc. Anti–c-myc antibody and tissue culture–treated chamber slides were obtained from BD.

Cytodex 3 beads, HRP-conjugated rabbit and mouse secondary antibodies, and ECL and ECL Plus kits were ordered from GE Healthcare. Dual Luciferase and caspase 3/7 assay kits were obtained from Promega. Labtek II chambered coverslips and all siRNA duplexes were purchased from Thermo Fisher Scientific.

Cell culture
Primary hPAECs from large vessels (Invitrogen; and ScienCell) were grown in EC media supplemented with 2% FBS, 1 µg/ml hydrocortisone, 10 ng/ml human epidermal growth factor, 3 ng/ml basic fibroblast growth factor, 10 µg/ml heparin, and gentamycin/amphotericin subcultured at a 1:4 ratio in 100-mm dishes (Corning) and used at passages 4–8. Cells were starved in Medium 200 with 0.1% FBS and gentamycin/amphotericin for 24 h before adding the agonist or the vehicle. Avoiding medium changes allows consistent determination of β-C and EC proliferation in response to the dose of BMP-2 used.

Proliferation assay
hPAECs were seeded at 25,000 cells per well on 24-well plates in growth medium and allowed to adhere overnight. Cells were washed three times with PBS and incubated in starvation media for 24 h followed by stimulation with agonists for 24 h. Cells were trypsinized and counted in a hemocytometer (Bright-Line; Hausser Scientific).

Survival assay
For caspase 3/7 assays, cells were seeded in a 96-well plate (4 wells per condition and 5,000 cells per well), allowed to attach overnight, and incubated for 24 h in serum-free media to induce apoptosis in the presence or absence of BMP-2 or Wnt3a. Cells were incubated for 1 h in 100 µl of Caspase 3/7 Luciferase Reagent Mix (Promega), and total luminescence was measured in a 20/20 luminometer (Turner Biosystems, Inc.).

Migration assay
Cytodex 3 cell culture beads were suspended in 1× PBS, autoclaved, and gently agitated in Petri dishes containing 10 ml of cell media followed by gentle agitation. Next, 1 ml hPAECs (10^5 cells/ml) was added and incubated overnight to allow attachment to the beads. Once cells had grown to confluence over the beads, 1 ml of cell-coated beads was added to a solution containing MEM and vitronectin, pH 7.6, and allowed to solidify. Cells were incubated for 30–60 min followed by the addition of 1.5 ml of cell media, with or without agonist, to the surface of each gel. After 48 h, cell migration was quantified by dividing each dish into four quadrants and selecting three beads in each for further analyses. Migration was quantified by the distance each cell traveled from the center of the bead. The mean distance traveled per quadrant was then used to calculate the mean distance migrated by cells in each plate. A microscope (DMRIRBA; Leica) with a headed channel switch Plan Apochromat 40× NA 0.85 objective was used.

Confocal microscopy
Cells were plated in four-chamber polystyrene glass slides (15,000 cells per chamber). For stimulation experiments, cells were starved for 24 h and stimulated with BMP as specified in the figure legends. Next, cells were fixed for 10 min in 4% paraformaldehyde followed by three washes with PBS. For experiments of native Dvl distribution in hPAECs, cells were permeabilized with ice-cold 1× PBS containing 0.1% Triton X-100 and donkey serum for 20 min followed by overnight incubation with goat anti-Dvl (Santa Cruz Biotechnology, Inc.) at RT, washed in 1× PBS, and incubated with Alexa Fluor 555 donkey anti–goat antibody (Invitrogen) for 1 h at RT followed by Alexa Fluor 488–labeled phalloidin for 20 min to stain actin filaments. For experiments of cells nucleofected with the various GFP-tagged Dvl constructs, actin staining was performed by incubating Alexa Fluor 555–phalloidin (Invitrogen) for 20 min after permeabilization with 0.1% Triton X-100 in PBS. Before mounting, slides were treated with Gold Antifade solution containing DAPI and stored at 4°C until analysis.

Confocal analysis was performed on a confocal laser-scanning microscope (SP2 AOBS; Leica) using a headed channel switch Plan Apochromat 63× NA 1.32–0.60 oil objective to locate areas of interest in the slides, and image acquisition was performed using the confocal build 1347 software (version 2.5; Leica) installed in the Leica confocal PC (Windows XP operating system). Images were processed and saved in JPEG format using Photoshop Creative Suite 2 (Adobe Systems).

To quantify distribution of GFP in PAECs transfected with the various Dvl constructs, GFP signal intensity in the cellular processes and the perinuclear area was measured in six randomly selected sectors using the ImageJ software (National Institutes of Health). A mean of the values was calculated, and a ratio of peripheral to central GFP intensity was plotted and used for statistical analyses. A total of four cells was used for each condition. The results were analyzed using Prism software (GraphPad Software, Inc.).

Western immunoblotting
hPAECs were washed three times with ice-cold 1× PBS, and lysates were prepared by adding boiling lysis buffer (10 mM Tris HCl, 1% SDS, and 0.2 mM PMSF) containing protease and phosphatase inhibitors, scraping into a 1.5-ml microcentrifuge tube, and boiling for 10 min before centrifugation. Supernatants were transferred to fresh microcentrifuge tubes and stored at −80°C. The protein concentration was determined by the Lowry assay (Bio-Rad Laboratories). Equal amounts of protein were loaded onto each lane of a 4–12% Bis-Tris gel and subjected to electrophoresis under reducing conditions. After blotting, polyvinylidene difluoride membranes were blocked for 1 h (5% milk powder in 0.1% TBS/Tween) and incubated with primary antibodies overnight at 4°C. The binding of secondary HRP antibodies was visualized by ECL or ECL Plus. Normalizing for total cell protein was performed by reprobing the membrane with a mouse monoclonal antibody against α-tubulin (Sigma-Aldrich).

Dvl plasmids and transfection methods
Plasmids encoding the WT, ΔDEP, ΔDIX, and DEP+ forms of Dvl were linked to a GFP tag and cloned in pCS vectors as described previously (Axelrod et al., 1998). An adenovirus containing a dominant-negative form of ERK1/2 was purchased from Seven Hills Bioreagents. Mutant constructs of Smad1 and Smad3 containing three serine to alanine substitutions in their C-terminal sequence and cloned in pCMV5 vectors were supplied by J. Massague (Memorial Sloan-Kettering Institute, New York, NY). Transfection of plasmids was performed using a Nucleofector II (program T-23) with the Basic Endothelial Cell Nucleofection kit (Amaxa, Inc.). All experiments were performed 24 h after nucleofection.

RNAi
To achieve gene knockdown, siRNA duplexes specific for β-C (On-Target Plus; Invitrogen; GenBank/EMBL/DDBJ accession no. NM_001012329 and NM_020248), ActRIIa (On-Target Plus; Invitrogen; GenBank/EMBL/DDBJ accession no. NM_001616), and BMPRII (On-Target Plus; Invitrogen; GenBank/EMBL/DDBJ accession no. NM_001204) were transfected into PAECs using nucleofection as described in the previous section. Knockdown efficiency was evaluated 48 h after nucleofection by measuring protein levels in cell lysates using a Western immunoblot.

Promoter-reporter assays
For measurements of β-C–mediated changes in gene expression, we used a TOPflash/FOPflash TCF/LEF reporter assay. The TOPflash construct contains a promoter with eight TCF/LEF1-binding domains found in the promoters of β-C target genes linked to a luciferase gene, whereas the FOPflash construct has mutated binding sites and serves as a negative control. hPAECs were transfected with either plasmid in a Nucleofector II (program T-23) using the Basic Endothelial Cell Nucleofection kit. After 24 h in starvation media, cells were stimulated, and luciferase production was measured 6 h later in a luminometer using the Dual Luciferase kit (Promega) according to the manufacturer's protocol. Renilla plasmid (Promega) cotransfection was used to control for transfection efficiency.

RhoA and Rac1 pull-down assays
hPAECs were washed three times with ice-cold 1× PBS. Cell lysates were prepared by adding 500 µl of ice-cold magnesium lysis buffer (10 mM Tris HCl, 1.0% SDS, 0.2 mM PMSF, and 100× protease and phosphatase inhibitor cocktails I and II; Millipore) to the cells and scraping into a 1.5-ml microcentrifuge tube on ice before cold centrifugation at 14,000 rpm for 10 min. Supernatants were transferred to fresh microcentrifuge tubes and stored at −80°C.

Active forms of RhoA or Rac1 were precipitated using glutathione beads containing rhotekin or PAK1, respectively, according to the manufacturer's protocol (Millipore). In brief, lysates were incubated with slurry containing the glutathione beads for 1 h at 4°C with constant rotation. At the end of this period, beads were precipitated by centrifuging lysates at 14,000 relative centrifuge force for 20 s. After washing three times with ice-cold buffer, beads were resuspended in Laemmli buffer, boiled, and subjected to Western immunoblot analysis as described above.

Digitally enhanced video differential interference contrast microscopy
48 h after transfection, cells were allowed to attach and spread on glass coverslips in the incubator and viewed on an inverted microscope

(Axiovert 35; Carl Zeiss, Inc.) with a Plan Apochromat 100× oil immersion lens (Carl Zeiss, Inc.) and a short distance condenser. The microscope is also equipped with a heated stage, differential interference contrast optics, and epifluorescence. Filters and light paths were controlled with a filter wheel and shutters (Ludl Electronic Products Ltd.). For GFP visualization, a single band excitation filter for FITC was used in combination with Pinkel#1 beam splitter and emission filter (Chroma Technology Corp.). Tissue culture medium without phenol red was kept warm and buffered in a CO_2 incubator. The stage temperature was kept at 37°C with an automatic thermostat. Images were collected using a charge-coupled device camera (C2400; B&W) with on-chip integration and a digital image processor (Argus 20; PerkinElmer). Acquired images were assembled in temporal sequences using Openlab software (PerkinElmer) and saved as QuickTime (Apple, Inc.) videos. The distance traveled by the cells was calculated by recording the position of the nucleus in individual frames using ImageJ software and plotting on an x–y axis followed by measurement of distance between each of the individual points. Total distance was obtained from the total sum of these values. Speed was measured by dividing total distance over time (10 h) using the following formula: S = D/t, where S = speed, D = distance and, t = time. A total of four cells was used for each measurement.

Matrigel plug angiogenesis assay in SCID mice

Animal experiments were approved by Stanford University's Institutional Review Board under the guidelines of the American Physiological Society. Matrigel plugs containing hPAECs were prepared as described previously (Skovseth et al., 2007), and 48 h after transfection, $\sim 1.0 \times 10^6$ cells were suspended in chilled 500 µl/plug of Matrigel Growth Factor Reduced solution (BD), to which recombinant BMP-2 diluted to a final concentration of 10 ng/ml or carrier was added. Plugs were implanted in the back of SCID mice (Charles River Laboratories) anesthetized by subcutaneous injection of a ketamine/xylazine cocktail. For each experimental condition, a total of four plugs was implanted in each animal and allowed to remain in place for 14 d. At the end of this period, the animals were humanely killed, and the solid Matrigel plugs were removed and fixed in 4% paraformaldehyde for 24 h and embedded in paraffin. Hematoxylin and eosin (H&E) sections were prepared. Unstained tissue samples were double labeled with Alexa Fluor 488–labeled anti–human CD31 and Alexa Fluor 555–labeled anti–mouse CD31 to identify human and murine ECs, respectively, along with DAPI to stain nuclei. 10 images per slide were captured using the 40× objective of an immunofluorescence microscope (DM RA2; Leica) and analyzed via Openlab software. The presence of microvessels (defined as tubes filled with red blood cells) was documented using H&E sections, and the number of human and murine cells per condition was quantified using the aforementioned immunofluorescence techniques.

Statistical analysis

Values from multiple experiments are expressed as mean ± SEM. Statistical significance was determined using one-way analysis of variance followed by Bonferroni's multiple comparison tests unless stated otherwise. A value of $P < 0.05$ was considered significant. The number of experiments and the sample number in each group are indicated in the figure legends.

Online supplemental material

Fig. S1 shows semiquantitative RT-PCR data for all 19 known Wnt ligands found in hPAECs at baseline. Fig. S2 shows confocal images of hPAECs stimulated with BMP-2 for 1 h and labeled with a primary antibody specific for β-C and an Alexa Fluor 488–labeled secondary antibody. Fig. S3 shows that hPAECs treated with BMPRII siRNA fail to accumulate β-C when stimulated with BMP-2, an event that correlates with failure to phosphorylate both ERK1/2 and GSK3-β. Fig. S4 shows the loss of BMP-2–mediated β-C accumulation and transcriptional activity in the presence of dominant-negative ERK (ΔERK). Fig. S5 demonstrates both the lack of impact of the Dvl mutant constructs on BMP-mediated β-C accumulation and the peripheral redistribution of Dvl in BMP-2– or Wnt3a-stimulated PAECs. Videos 1 and 2 show hPAECs transfected with WT Dvl at baseline (Video 1) and in the presence of BMP-2 (Video 2). Videos 3 and 4 show hPAECs transfected with ΔDEP exposed to the same conditions as described for Videos 1 and 2. Online supplemental material is available at http://www.jcb.org/cgi/content/full/jcb.200806049/DC1.

We would like to thank Dr. Michal Bental Roof for her invaluable help in the preparation of the figures for this manuscript and to Drs. Roel Nusse, David Cornfield, and Glenn Rosen at Stanford University for their helpful scientific discussions. We also thank Qicong Hu, who helped in the compression of the video files for this submission.

This work was supported by National Institutes of Health grant R01 HL074186 to M. Rabinovitch and by an endowment of the Wall Center for Pulmonary Vascular Diseases at Stanford University. V.A. de Jesus Perez was funded by both the National Institutes of Health T32 Training Grant and American Lung Association Postdoctoral Fellowship. J.D. Axelrod was supported by the National Institutes of Health grant R01GM059823. T.-P. Alastalo was funded by postdoctoral fellowships from the Sigrid Juselius Foundation, Instrumentarium Foundation, the Finnish Foundation for Cardiovascular Research, and the Academy of Finland.

Submitted: 9 June 2008
Accepted: 11 December 2008

References

Adams, R.H., and K. Alitalo. 2007. Molecular regulation of angiogenesis and lymphangiogenesis. *Nat. Rev. Mol. Cell Biol.* 8:464–478.

Asosingh, K., M.A. Aldred, A. Vasanji, J. Drazba, J. Sharp, C. Farver, S.A. Comhair, W. Xu, L. Licina, L. Huang, et al. 2008. Circulating angiogenic precursors in idiopathic pulmonary arterial hypertension. *Am. J. Pathol.* 172:615–627.

Attisano, L., and J.L. Wrana. 2002. Signal transduction by the TGF-beta superfamily. *Science*. 296:1646–1647.

Axelrod, J.D., and H. McNeill. 2002. Coupling planar cell polarity signaling to morphogenesis. *ScientificWorldJournal*. 2:434–454.

Axelrod, J.D., J.R. Miller, J.M. Shulman, R.T. Moon, and N. Perrimon. 1998. Differential recruitment of Dishevelled provides signaling specificity in the planar cell polarity and Wingless signaling pathways. *Genes Dev.* 12:2610–2622.

Bain, G., T. Muller, X. Wang, and J. Papkoff. 2003. Activated beta-catenin induces osteoblast differentiation of C3H10T1/2 cells and participates in BMP2 mediated signal transduction. *Biochem. Biophys. Res. Commun.* 301:84–91.

Beppu, H., M. Kawabata, T. Hamamoto, A. Chytil, O. Minowa, T. Noda, and K. Miyazono. 2000. BMP type II receptor is required for gastrulation and early development of mouse embryos. *Dev. Biol.* 221:249–258.

Boutros, M., N. Paricio, D.I. Strutt, and M. Mlodzik. 1998. Dishevelled activates JNK and discriminates between JNK pathways in planar polarity and wingless signaling. *Cell*. 94:109–118.

Capelluto, D.G., T.G. Kutateladze, R. Habas, C.V. Finkielstein, X. He, and M. Overduin. 2002. The DIX domain targets dishevelled to actin stress fibres and vesicular membranes. *Nature*. 419:726–729.

Chen, C., H. Chen, J. Sun, P. Bringas Jr., Y. Chen, D. Warburton, and W. Shi. 2005. Smad1 expression and function during mouse embryonic lung branching morphogenesis. *Am. J. Physiol. Lung Cell. Mol. Physiol.* 288: L1033–L1039.

Cohen, P., and S. Frame. 2001. The renaissance of GSK3. *Nat. Rev. Mol. Cell Biol.* 2:769–776.

Cottin, V., S. Dupuis-Girod, G. Lesca, and J.F. Cordier. 2007. Pulmonary vascular manifestations of hereditary hemorrhagic telangiectasia (rendu-osler disease). *Respiration*. 74:361–378.

Date, T., Y. Doiguchi, M. Nobuta, and H. Shindo. 2004. Bone morphogenetic protein-2 induces differentiation of multipotent C3H10T1/2 cells into osteoblasts, chondrocytes, and adipocytes in vivo and in vitro. *J. Orthop. Sci.* 9:503–508.

Deckers, M.M., R.L. van Bezooijen, G. van der Horst, J. Hoogendam, C. van Der Bent, S.E. Papapoulos, and C.W. Lowik. 2002. Bone morphogenetic proteins stimulate angiogenesis through osteoblast-derived vascular endothelial growth factor A. *Endocrinology*. 143:1545–1553.

Deng, Z., J.H. Morse, S.L. Slager, N. Cuervo, K.J. Moore, G. Venetos, S. Kalachikov, E. Cayanis, S.G. Fischer, R.J. Barst, et al. 2000. Familial primary pulmonary hypertension (gene PPH1) is caused by mutations in the bone morphogenetic protein receptor-II gene. *Am. J. Hum. Genet.* 67:737–744.

Ding, Q., W. Xia, J.C. Liu, J.Y. Yang, D.F. Lee, J. Xia, G. Bartholomeusz, Y. Li, Y. Pan, Z. Li, et al. 2005. Erk associates with and primes GSK-3beta for its inactivation resulting in upregulation of beta-catenin. *Mol. Cell*. 19:159–170.

Endo, Y., V. Wolf, K. Muraiso, K. Kamijo, L. Soon, A. Uren, M. Barshishat-Kupper, and J.S. Rubin. 2005. Wnt-3a-dependent cell motility involves RhoA activation and is specifically regulated by dishevelled-2. *J. Biol. Chem.* 280:777–786.

Fischer, L., G. Boland, and R.S. Tuan. 2002. Wnt signaling during BMP-2 stimulation of mesenchymal chondrogenesis. *J. Cell. Biochem.* 84:816–831.

Foletta, V.C., M.A. Lim, J. Soosairajah, A.P. Kelly, E.G. Stanley, M. Shannon, W. He, S. Das, J. Massague, and O. Bernard. 2003. Direct signaling by

the BMP type II receptor via the cytoskeletal regulator LIMK1. *J. Cell Biol.* 162:1089–1098.

Glinka, A., W. Wu, H. Delius, A.P. Monaghan, C. Blumenstock, and C. Niehrs. 1998. Dickkopf-1 is a member of a new family of secreted proteins and functions in head induction. *Nature*. 391:357–362.

Habas, R., I.B. Dawid, and X. He. 2003. Coactivation of Rac and Rho by Wnt/Frizzled signaling is required for vertebrate gastrulation. *Genes Dev.* 17:295–309.

Hansmann, G., R.A. Wagner, S. Schellong, V.A. Perez, T. Urashima, L. Wang, A.Y. Sheikh, R.S. Suen, D.J. Stewart, and M. Rabinovitch. 2007. Pulmonary arterial hypertension is linked to insulin resistance and reversed by peroxisome proliferator-activated receptor-gamma activation. *Circulation*. 115:1275–1284.

He, T.C., A.B. Sparks, C. Rago, H. Hermeking, L. Zawel, L.T. da Costa, P.J. Morin, B. Vogelstein, and K.W. Kinzler. 1998. Identification of c-MYC as a target of the APC pathway. *Science*. 281:1509–1512.

Hu, M.C., and N.D. Rosenblum. 2005. Smad1, beta-catenin and Tcf4 associate in a molecular complex with the Myc promoter in dysplastic renal tissue and cooperate to control Myc transcription. *Development*. 132:215–225.

Humbert, M., N.W. Morrell, S.L. Archer, K.R. Stenmark, M.R. MacLean, I.M. Lang, B.W. Christman, E.K. Weir, O. Eickelberg, N.F. Voelkel, and M. Rabinovitch. 2004a. Cellular and molecular pathobiology of pulmonary arterial hypertension. *J. Am. Coll. Cardiol.* 43:13S–24S.

Humbert, M., O. Sitbon, and G. Simonneau. 2004b. Treatment of pulmonary arterial hypertension. *N. Engl. J. Med.* 351:1425–1436.

Ishikawa, T., Y. Tamai, A.M. Zorn, H. Yoshida, M.F. Seldin, S. Nishikawa, and M.M. Taketo. 2001. Mouse Wnt receptor gene Fzd5 is essential for yolk sac and placental angiogenesis. *Development*. 128:25–33.

Ishitani, T., J. Ninomiya-Tsuji, S. Nagai, M. Nishita, M. Meneghini, N. Barker, M. Waterman, B. Bowerman, H. Clevers, H. Shibuya, and K. Matsumoto. 1999. The TAK1-NLK-MAPK-related pathway antagonizes signalling between beta-catenin and transcription factor TCF. *Nature*. 399:798–802.

Ishitani, T., J. Ninomiya-Tsuji, and K. Matsumoto. 2003. Regulation of lymphoid enhancer factor 1/T-cell factor by mitogen-activated protein kinase-related Nemo-like kinase-dependent phosphorylation in Wnt/beta-catenin signaling. *Mol. Cell. Biol.* 23:1379–1389.

Jin, E.J., S.Y. Lee, Y.A. Choi, J.C. Jung, O.S. Bang, and S.S. Kang. 2006. BMP-2-enhanced chondrogenesis involves p38 MAPK-mediated down-regulation of Wnt-7a pathway. *Mol. Cells*. 22:353–359.

Kishida, S., H. Yamamoto, and A. Kikuchi. 2004. Wnt-3a and Dvl induce neurite retraction by activating Rho-associated kinase. *Mol. Cell. Biol.* 24:4487–4501.

Labbe, E., A. Letamendia, and L. Attisano. 2000. Association of Smads with lymphoid enhancer binding factor 1/T cell-specific factor mediates cooperative signaling by the transforming growth factor-beta and wnt pathways. *Proc. Natl. Acad. Sci. USA*. 97:8358–8363.

Lamalice, L., F. Le Boeuf, and J. Huot. 2007. Endothelial cell migration during angiogenesis. *Circ. Res.* 100:782–794.

Langenfeld, E.M., and J. Langenfeld. 2004. Bone morphogenetic protein-2 stimulates angiogenesis in developing tumors. *Mol. Cancer Res.* 2:141–149.

Li, L., H. Yuan, W. Xie, J. Mao, A.M. Caruso, A. McMahon, D.J. Sussman, and D. Wu. 1999. Dishevelled proteins lead to two signaling pathways. Regulation of LEF-1 and c-Jun N-terminal kinase in mammalian cells. *J. Biol. Chem.* 274:129–134.

Liu, Z., Y. Tang, T. Qiu, X. Cao, and T.L. Clemens. 2006. A dishevelled-1/Smad1 interaction couples WNT and bone morphogenetic protein signaling pathways in uncommitted bone marrow stromal cells. *J. Biol. Chem.* 281:17156–17163.

Logan, C.Y., and R. Nusse. 2004. The Wnt signaling pathway in development and disease. *Annu. Rev. Cell Dev. Biol.* 20:781–810.

Long, L., M.R. MacLean, T.K. Jeffery, I. Morecroft, X. Yang, N. Rudarakanchana, M. Southwood, V. James, R.C. Trembath, and N.W. Morrell. 2006. Serotonin increases susceptibility to pulmonary hypertension in BMPR2-deficient mice. *Circ. Res.* 98:818–827.

Machado, R.D., M.W. Pauciulo, J.R. Thomson, K.B. Lane, N.V. Morgan, L. Wheeler, J.A. Phillips III, J. Newman, D. Williams, N. Galie, et al. 2001. BMPR2 haploinsufficiency as the inherited molecular mechanism for primary pulmonary hypertension. *Am. J. Hum. Genet.* 68:92–102.

Machado, R.D., N. Rudarakanchana, C. Atkinson, J.A. Flanagan, R. Harrison, N.W. Morrell, and R.C. Trembath. 2003. Functional interaction between BMPR-II and Tctex-1, a light chain of Dynein, is isoform-specific and disrupted by mutations underlying primary pulmonary hypertension. *Hum. Mol. Genet.* 12:3277–3286.

Masckauchan, T.N., C.J. Shawber, Y. Funahashi, C.M. Li, and J. Kitajewski. 2005. Wnt/beta-catenin signaling induces proliferation, survival and interleukin-8 in human endothelial cells. *Angiogenesis*. 8:43–51.

Masri, F.A., W. Xu, S.A. Comhair, K. Asosingh, M. Koo, A. Vasanji, J. Drazba, B. Anand-Apte, and S.C. Erzurum. 2007. Hyperproliferative apoptosis-resistant endothelial cells in idiopathic pulmonary arterial hypertension. *Am. J. Physiol. Lung Cell. Mol. Physiol.* 293:L548–L554.

Massague, J. 2003. Integration of Smad and MAPK pathways: a link and a linker revisited. *Genes Dev.* 17:2993–2997.

Mishina, Y., A. Suzuki, N. Ueno, and R.R. Behringer. 1995. Bmpr encodes a type I bone morphogenetic protein receptor that is essential for gastrulation during mouse embryogenesis. *Genes Dev.* 9:3027–3037.

Miyazono, K., and K. Miyazawa. 2002. Id: a target of BMP signaling. *Sci. STKE.* doi:10.1126/stke.2002.151.pe40.

Moriguchi, T., K. Kawachi, S. Kamakura, N. Masuyama, H. Yamanaka, K. Matsumoto, A. Kikuchi, and E. Nishida. 1999. Distinct domains of mouse dishevelled are responsible for the c-Jun N-terminal kinase/stress-activated protein kinase activation and the axis formation in vertebrates. *J. Biol. Chem.* 274:30957–30962.

Moule, S.K., G.I. Welsh, N.J. Edgell, E.J. Foulstone, C.G. Proud, and R.M. Denton. 1997. Regulation of protein kinase B and glycogen synthase kinase-3 by insulin and beta-adrenergic agonists in rat epididymal fat cells. Activation of protein kinase B by wortmannin-sensitive and -insensitive mechanisms. *J. Biol. Chem.* 272:7713–7719.

Nusse, R., and H.E. Varmus. 1992. Wnt genes. *Cell*. 69:1073–1087.

Peifer, M. 1997. Beta-catenin as oncogene: the smoking gun. *Science*. 275: 1752–1753.

Raida, M., J.H. Clement, R.D. Leek, K. Ameri, R. Bicknell, D. Niederwieser, and A.L. Harris. 2005. Bone morphogenetic protein 2 (BMP-2) and induction of tumor angiogenesis. *J. Cancer Res. Clin. Oncol.* 131:741–750.

Rawadi, G., B. Vayssiere, F. Dunn, R. Baron, and S. Roman-Roman. 2003. BMP-2 controls alkaline phosphatase expression and osteoblast mineralization by a Wnt autocrine loop. *J. Bone Miner. Res.* 18:1842–1853.

Rich, S., D.R. Dantzker, S.M. Ayres, E.H. Bergofsky, B.H. Brundage, K.M. Detre, A.P. Fishman, R.M. Goldring, B.M. Groves, S.K. Koerner, et al. 1987. Primary pulmonary hypertension. A national prospective study. *Ann. Intern. Med.* 107:216–223.

Roberts, K.E., J.J. McElroy, W.P. Wong, E. Yen, A. Widlitz, R.J. Barst, J.A. Knowles, and J.H. Morse. 2004. BMPR2 mutations in pulmonary arterial hypertension with congenital heart disease. *Eur. Respir. J.* 24:371–374.

Sakao, S., L. Taraseviciene-Stewart, K. Wood, C.D. Cool, and N.F. Voelkel. 2006. Apoptosis of pulmonary microvascular endothelial cells stimulates vascular smooth muscle cell growth. *Am. J. Physiol. Lung Cell. Mol. Physiol.* 291:L362–L368.

Sandquist, J.C., K.I. Swenson, K.A. Demali, K. Burridge, and A.R. Means. 2006. Rho kinase differentially regulates phosphorylation of nonmuscle myosin II isoforms A and B during cell rounding and migration. *J. Biol. Chem.* 281:35873–35883.

Seki, K., and A. Hata. 2004. Indian hedgehog gene is a target of the bone morphogenetic protein signaling pathway. *J. Biol. Chem.* 279:18544–18549.

Skovseth, D.K., T. Yamanaka, P. Brandtzaeg, E.C. Butcher, and G. Haraldsen. 2002. Vascular morphogenesis and differentiation after adoptive transfer of human endothelial cells to immunodeficient mice. *Am. J. Pathol.* 160:1629–1637.

Skovseth, D.K., A.M. Kuchler, and G. Haraldsen. 2007. The HUVEC/Matrigel assay: an in vivo assay of human angiogenesis suitable for drug validation. *Methods Mol. Biol.* 360:253–268.

Song, Y., J.E. Jones, H. Beppu, J.F. Keaney Jr., J. Loscalzo, and Y.Y. Zhang. 2005. Increased susceptibility to pulmonary hypertension in heterozygous BMPR2-mutant mice. *Circulation*. 112:553–562.

Sugimori, K., K. Matsui, H. Motomura, T. Tokoro, J. Wang, S. Higa, T. Kimura, and I. Kitajima. 2005. BMP-2 prevents apoptosis of the N1511 chondrocytic cell line through PI3K/Akt-mediated NF-kappaB activation. *J. Bone Miner. Metab.* 23:411–419.

Suzuki, K., D. Bachiller, Y.P. Chen, M. Kamikawa, H. Ogi, R. Haraguchi, Y. Ogino, Y. Minami, Y. Mishina, K. Ahn, et al. 2003. Regulation of outgrowth and apoptosis for the terminal appendage: external genitalia development by concerted actions of BMP signaling. *Development*. 130:6209–6220.

Tang, S.J., P.A. Hoodless, Z. Lu, M.L. Breitman, R.R. McInnes, J.L. Wrana, and M. Buchwald. 1998. The Tlx-2 homeobox gene is a downstream target of BMP signalling and is required for mouse mesoderm development. *Development*. 125:1877–1887.

Teichert-Kuliszewska, K., M.J. Kutryk, M.A. Kuliszewski, G. Karoubi, D.W. Courtman, L. Zucco, J. Granton, and D.J. Stewart. 2006. Bone morphogenetic protein receptor-2 signaling promotes pulmonary arterial endothelial cell survival: implications for loss-of-function mutations in the pathogenesis of pulmonary hypertension. *Circ. Res.* 98:209–217.

Tetsu, O., and F. McCormick. 1999. Beta-catenin regulates expression of cyclin D1 in colon carcinoma cells. *Nature*. 398:422–426.

Thomson, J.R., R.D. Machado, M.W. Pauciulo, N.V. Morgan, M. Humbert, G.C. Elliott, K. Ward, M. Yacoub, G. Mikhail, P. Rogers, et al. 2000. Sporadic primary pulmonary hypertension is associated with germline mutations of the gene encoding BMPR-II, a receptor member of the TGF-beta family. *J. Med. Genet.* 37:741–745.

Thornton, T.M., G. Pedraza-Alva, B. Deng, C.D. Wood, A. Aronshtam, J.L. Clements, G. Sabio, R.J. Davis, D.E. Matthews, B. Doble, and M. Rincon. 2008. Phosphorylation by p38 MAPK as an alternative pathway for GSK3beta inactivation. *Science*. 320:667–670.

Torres, M.A., and W.J. Nelson. 2000. Colocalization and redistribution of dishevelled and actin during Wnt-induced mesenchymal morphogenesis. *J. Cell Biol.* 149:1433–1442.

Tuder, R.M., and N.F. Voelkel. 2002. Angiogenesis and pulmonary hypertension: a unique process in a unique disease. *Antioxid. Redox Signal.* 4:833–843.

van Nieuw Amerongen, G.P., and V.W. van Hinsbergh. 2001. Cytoskeletal effects of rho-like small guanine nucleotide-binding proteins in the vascular system. *Arterioscler. Thromb. Vasc. Biol.* 21:300–311.

Wang, J., N.S. Hamblet, S. Mark, M.E. Dickinson, B.C. Brinkman, N. Segil, S.E. Fraser, P. Chen, J.B. Wallingford, and A. Wynshaw-Boris. 2006. Dishevelled genes mediate a conserved mammalian PCP pathway to regulate convergent extension during neurulation. *Development*. 133:1767–1778.

Warner, D.R., R.M. Greene, and M.M. Pisano. 2005. Interaction between Smad 3 and Dishevelled in murine embryonic craniofacial mesenchymal cells. *Orthod. Craniofac. Res.* 8:123–130.

Wright, M., M. Aikawa, W. Szeto, and J. Papkoff. 1999. Identification of a Wnt-responsive signal transduction pathway in primary endothelial cells. *Biochem. Biophys. Res. Commun.* 263:384–388.

Yamaguchi, K., K. Shirakabe, H. Shibuya, K. Irie, I. Oishi, N. Ueno, T. Taniguchi, E. Nishida, and K. Matsumoto. 1995. Identification of a member of the MAPKKK family as a potential mediator of TGF-beta signal transduction. *Science*. 270:2008–2011.

Yang, N., O. Higuchi, K. Ohashi, K. Nagata, A. Wada, K. Kangawa, E. Nishida, and K. Mizuno. 1998. Cofilin phosphorylation by LIM-kinase 1 and its role in Rac-mediated actin reorganization. *Nature*. 393:809–812.

Yang, X., L. Long, M. Southwood, N. Rudarakanchana, P.D. Upton, T.K. Jeffery, C. Atkinson, H. Chen, R.C. Trembath, and N.W. Morrell. 2005. Dysfunctional Smad signaling contributes to abnormal smooth muscle cell proliferation in familial pulmonary arterial hypertension. *Circ. Res.* 96:1053–1063.

Yeager, M.E., G.R. Halley, H.A. Golpon, N.F. Voelkel, and R.M. Tuder. 2001. Microsatellite instability of endothelial cell growth and apoptosis genes within plexiform lesions in primary pulmonary hypertension. *Circ. Res.* 88:E2–E11.

Yu, A., J.F. Rual, K. Tamai, Y. Harada, M. Vidal, X. He, and T. Kirchhausen. 2007. Association of Dishevelled with the clathrin AP-2 adaptor is required for Frizzled endocytosis and planar cell polarity signaling. *Dev. Cell*. 12:129–141.

Yu, P.B., H. Beppu, N. Kawai, E. Li, and K.D. Bloch. 2005. Bone morphogenetic protein (BMP) type II receptor deletion reveals BMP ligand-specific gain of signaling in pulmonary artery smooth muscle cells. *J. Biol. Chem.* 280:24443–24450.

Zhang, T., T. Otevrel, Z. Gao, Z. Gao, S.M. Ehrlich, J.Z. Fields, and B.M. Boman. 2001a. Evidence that APC regulates survivin expression: a possible mechanism contributing to the stem cell origin of colon cancer. *Cancer Res.* 61:8664–8667.

Zhang, X., J.P. Gaspard, and D.C. Chung. 2001b. Regulation of vascular endothelial growth factor by the Wnt and K-ras pathways in colonic neoplasia. *Cancer Res.* 61:6050–6054.